



**TECHNISCHE
UNIVERSITÄT
DRESDEN**

DLR Design Challenge 2022

PEL-E-FAN-T

proPELLor driven turbo Electric hybrid Firefighting AutoNomous vTol



Team

P. Sanderbrand, L. Köhler, M. Wenk, H. Jerzembek, D. Brunner

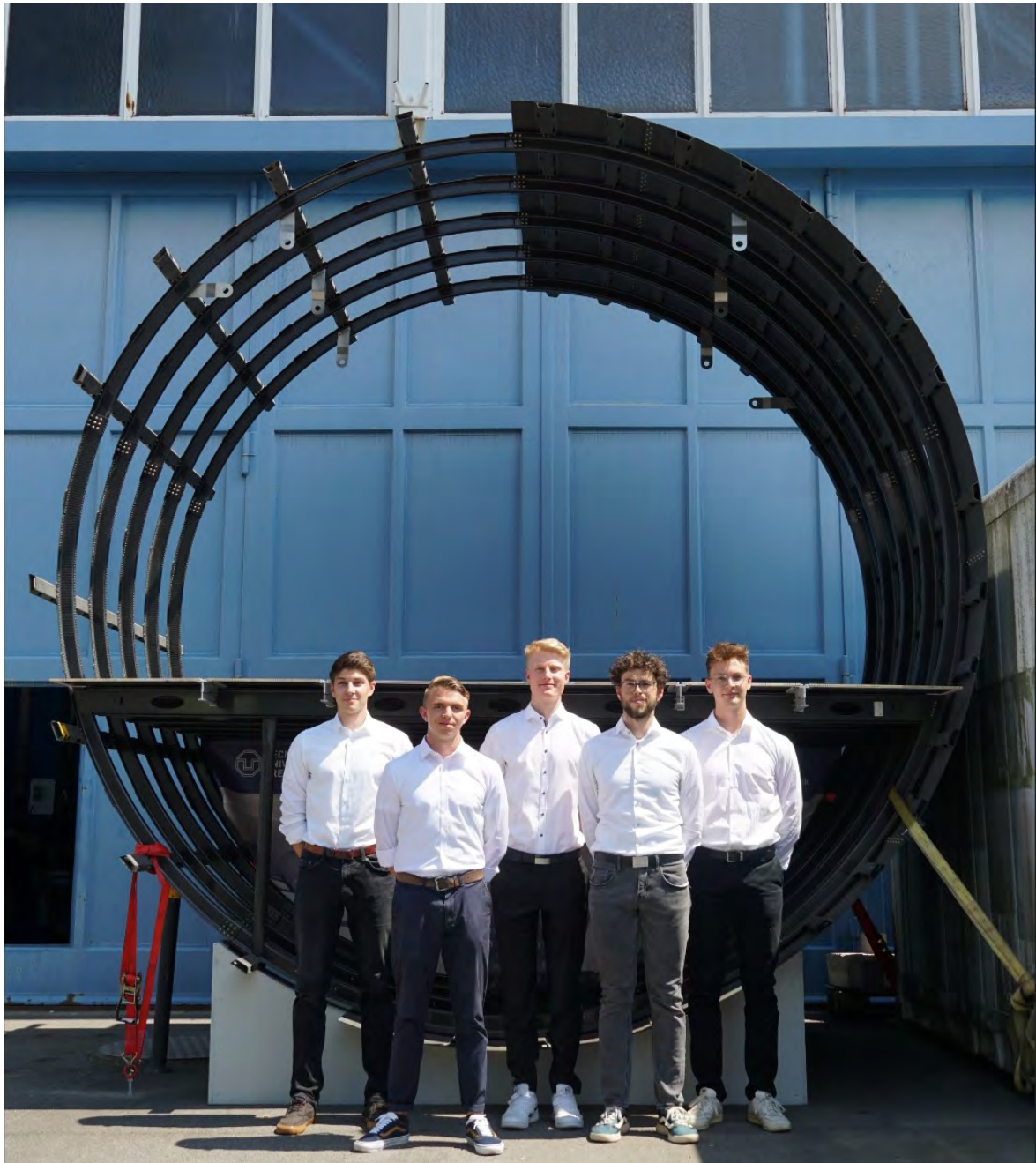
Academic Support

Dipl.-Ing. Florian Dextl
Chair of Aircraft Engineering
Technische Universität Dresden

Submission Date

July 11th, 2022

Team Members



Team members from left to right:

H. Jerzembek, P. Sanderbrand, M. Wenk, L. Köhler, D. Brunner

Student Information

Hannes Jerzembek

Aerospace Engineering, 6th semester (Diploma)
Hannes.Jerzembek@mailbox.tu-dresden.de

Paul Sanderbrand

Aerospace Engineering, 6th semester (Diploma)
Paul.Sanderbrand@mailbox.tu-dresden.de

Maximilian Wenk

Aerospace Engineering, 6th semester (Diploma)
Maximilian.Wenk@mailbox.tu-dresden.de

Lennard Köhler

Aerospace Engineering, 6th semester (Diploma)
Lennard.Köhler@mailbox.tu-dresden.de

Dominik Brunner

Aerospace Engineering, 6th semester (Diploma)
Dominik.Brunner@mailbox.tu-dresden.de



Deutsches Zentrum für Luft- und Raumfahrt e. V. (DLR)
Institut für Systemarchitekturen in der Luftfahrt | Automatisierung, Energie und Sicherheit

Prof. Dr.
Johannes Markmiller
Professur für Luftfahrzeugtechnik
Bearbeitung: Florian Dexl
Wissenschaftlicher Mitarbeiter
Telefon: 0351 463-38096
Telefax: 0351 463-37263
E-Mail: florian.dexl@tu-dresden.de
AZ: 22-08
Datum: 11.07.2022

NASA/DLR Design Challenge: Approval and support of report submission

To whom it may concern,

As the academic supervisors, we hereby declare to approve the report written by the student team consisting of:

- Dominik Brunner,
- Hannes Jerzembek,
- Lennard Köhler,
- Paul Sanderbrand,
- Max Wenk

and support the submission to the NASA/DLR Design Challenge 2022. We further declare that the report is the result of the above-listed students' own work.

Best regards



Institut für Luft- und Raumfahrttechnik
Professur für Luftfahrzeugtechnik
Prof. Dr. Johannes Markmiller
01062 Dresden

Prof. Dr. Johannes Markmiller



Dipl.-Ing. Florian Dexl

Briefadresse

TU Dresden,
Professur für Luftfahrzeugtechnik
01062 Dresden

Besuchsadresse

Marschnerstr. 32
Raum 316

**Steuernummer
(Inland)**

203/149/02549

Bankverbindung

Commerzbank AG,
Filiale Dresden

Die TU Dresden ist
Partner im Netzwerk
DRESDEN-concept

Paketadresse

TU Dresden,
Professur für Luftfahrzeugtechnik
Helmholtzstr. 10

Kein barrierefreier Zugang

Umsatzsteuer-Id-Nr.

(Ausland)
DE 188 369 991

IBAN

DE52 8504 0000 0800 4004 00

BIC

COBADEFF850

**DRESDEN
concept**



Abstract

Wildfires pose an increasing threat to humans and wildlife in Europe as climate change further intensifies fire conducive weather, growing the burnt area and economic damage year after year. That's why, the DLR Design Challenge 2022 appointed students with the task to design an efficient, economically reasonable, safe, reliable, and quiet fleet of firefighting aircraft on the existing foundation of a UAM- or RAM- vehicle. The Propellor Driven Electric Firefighting Autonomous VTOL (PEL-E-FAN-T) presents an excellent solution to the task. As a fixed-wing VTOL the aircraft, designed by the team of TU Dresden, combines the cruise flight advantages of a traditional aircraft with the vertical take-off capabilities of a VTOL whilst minimizing danger for human life by operating without a pilot on board. The hybrid-electric powertrain provides a satisfying range while making VTOL capabilities possible in the first place. Utilizing a canard configuration the concept features high maneuverability. One of the key features is a modular design, providing a significant advantage to a traditional retrofit both economically and in terms of work hours. Additionally with one airframe, firefighting, cargo, and passenger configuration are possible, which is also useful in firefighting situations e.g. to evacuate encircled people.

Waldbrände stellen eine zunehmende Bedrohung für Menschen und Wildtiere in Europa dar, da der Klimawandel das feuerfördernde Wetter weiter verschärft, die verbrannte Fläche vergrößert und Jahr für Jahr wirtschaftlichen Schaden anrichtet. Aus diesen Gründen hat die DLR Design Challenge 2022 Studenten mit der Aufgabe beauftragt, auf dem bestehenden Fundament eines UAM- oder RAM-Fahrzeugs eine effiziente, wirtschaftlich sinnvolle, sichere, zuverlässige und leise Flotte von Löschflugzeugen zu entwerfen. Das Propeller Driven Electric Firefighting Autonomous VTOL (PEL-E-FAN-T) bietet eine hervorragende Lösung für diese Aufgabe. Als fixed-wing VTOL kombiniert das vom Team der TU Dresden konzipierte Flugzeug die Reiseflugvorteile eines traditionellen Flugzeugs mit den Senkrechtstartfähigkeiten eines VTOL und minimiert die Gefahr für Menschenleben, indem es ohne Pilot an Bord arbeitet. Der hybrid-elektrische Antriebsstrang bietet eine zufriedenstellende Reichweite und macht die VTOL-Fähigkeiten des Konzepts überhaupt erst möglich. Durch die Verwendung einer Canard-Konfiguration zeichnet sich das Konzept durch eine hohe Manövrierfähigkeit aus. Eines der Hauptmerkmale ist ein modularer Aufbau, der sowohl wirtschaftlich als auch in Bezug auf die Arbeitszeit einen erheblichen Vorteil gegenüber einer herkömmlichen Nachrüstung bietet. Zusätzlich sind mit einer Flugzeugzelle Brandbekämpfungs-, Fracht- und Passagierkonfiguration möglich, was auch in Brandbekämpfungssituationen nützlich ist, beispielsweise um eingekreiste Personen zu evakuieren.

Contents

Nomenclature	IV
List of Figures	VIII
List of Tables	VIII
1 Introduction and Analysis of the status quo	1
2 Concept Summary	2
2.1 Concept Overview	2
2.2 Key Technologies	3
2.3 Evaluation	3
2.3.1 Safety and Failure Modes	3
2.3.2 Fulfillment of Requirements	4
3 Design Overview	4
3.1 Aircraft Design	5
3.2 Hybrid-electric Powertrain	5
3.2.1 Mechanical link	6
3.2.2 Power and Energy demand	6
3.2.3 Comparison with conventional firefighting aircraft	9
3.2.4 Battery and system architecture	10
3.3 Modules	11
3.3.1 Firefighting Configuration	11
3.3.2 Cargo Configuration	12
3.3.3 Evacuation Configuration	12
3.3.4 Passenger Configuration	12
3.4 Aerodynamics	13
3.4.1 Wing	13
3.4.2 Canard and vertical stabilizer	13
3.4.3 Drag estimation	14
3.5 Shifting CG	14
3.6 Mass	14
4 Avionics and Autonomy	16
4.1 Single Pilot Operation	16
4.2 Autonomous Flight	16
4.2.1 Hardware	17
4.2.2 Software	17
5 Operational Concept	19
5.1 Fleet Size	19
5.2 Fleet-Type	19
5.3 Tactics	19
5.3.1 Traditional Tactics	19
5.4 Ground Handling	20
5.5 Design Mission	22
5.5.1 Inland Scenario	23
5.5.2 Seaside Scenario	23

5.6	Further Uses	24
6	Cost Estimation	25
6.1	Life Cycle Costs	25
6.2	Impact of Autonomy	25
7	Conclusion	25
	References	26
A	Appendix	i
A.1	Formulas	i
A.1.1	power and energy demand formulas	i
A.1.2	aerodynamic formulas	i
A.1.3	mass estimation formulas	i
A.2	Aircraft and Mission Data	iii
A.3	Constants	iv
A.4	Equation Results	v
A.5	Mass aircraft components	vi
A.6	Figures	vii

Nomenclature

Abbreviations

AOC	Airline-Operating Center
AS	Assistant Systems
CO ₂	Carbon Dioxide
CG	Center of Gravity
CIF	Climbing Flight
CrF	Cruise Flight
DL	Disc Loading
EM	Electric motor
EIS	Entry Into Service
EASA	European Union Aviation Safety Agency
GO	Ground Operator
HO	Hover Flight
IMU	Internal Measurement Unit
ISA	International Standard Atmosphere
L	Landing
L/D	Lift-to-Drag
PIC	Pilot in Command
R	Reserve
RPM	Rotations per Minute
SPO	Single Pilot Operation
TC	Taxonomy of operating Conditions
TRL	Technology Readiness Level
TO	Take Off
TE	Total Energy
T _{ch}	Transition cruise to hover
T _{hc}	Transition hover to cruise
UAV	Unmanned Aerial Vehicle
UAS	Unmanned Aircraft System
VC	Vertical Climb
VD	Vertical Descent

Symbol	Description	Unit
S_{HT}	area horizontal tail	$[m^2]$
S_{VT}	area vertical tail	$[m^2]$
v_{climb}	climb velocity	$[\frac{m}{s}]$
$v_{climb,sc}$	climb velocity service ceiling	$[\frac{m}{s}]$
t_{climb}	climb time	$[s]$
P_{climb}	climb power	$[MW]$
$P_{climb,sc}$	climb power service ceiling	$[MW]$
k	constant for induced velocity	$[-]$
k_1	constant for induced velocity	$[-]$

k_2	constant for induced velocity	[-]
k_3	constant for induced velocity	[-]
k_4	constant for induced velocity	[-]
P_{cruise}	cruise power	[MW]
v_{cruise}	cruise velocity	$[\frac{m}{s}]$
v_{descent}	descent velocity	$[\frac{m}{s}]$
v_d	descent velocity in transition	$[\frac{m}{s}]$
C_D	drag coefficient	[-]
$E_{\text{density,battery}}$	energy density battery	$[\frac{Wh}{kg}]$
$E_{\text{density,kerosin}}$	energy density kerosin	$[\frac{kWh}{kg}]$
$m_{\text{eng,ff}}$	engine mass for forward flight	[kg]
$m_{\text{eng,vtol}}$	engine mass for vtol	[kg]
t_{fillup}	fillup time	[s]
d_{fus}	diameter fuselage	[m]
m_{fus}	fuselage mass for aircraft, cargo and water module	[kg]
g	gravitational acceleration	$[\frac{m}{s^2}]$
W_0	gravitational force	[N]
H	height	[mm]
h_{fus}	height of fuselage	[m]
H_{base}	height of the operational Base above Sea Level	[m]
H_w	height of the water reservoir above Sea Level	[m]
H_{sc}	height service ceiling	[m]
c_{HT}	horizontal tail volume coefficient	[-]
P_{hover}	hover power	[MW]
t_{hover}	hover time	[s]
v_h	induced velocity	$[\frac{m}{s}]$
$v_{i,\text{desc}}$	induced vertical descent velocity	$[\frac{m}{s}]$
$v_{i,\text{ld}}$	induced vertical landing velocity	$[\frac{m}{s}]$
m_{land}	landing gear mass	[kg]
s_{land}	landing distance	[m]
L	length	[mm]
l_{fus}	length of fuselage	[m]
C_L	lift coefficient	[-]
$\Delta c_{a,\text{max,hld,to}}$	lift coefficient triple slotted flap with slotted leading edge flap, take off	[-]
$\Delta c_{a,\text{max,hld,l}}$	lift coefficient triple slotted flap with slotted leading edge flap, landing	[-]
$C_{L\alpha}$	lift gradient	[-]
$\frac{L}{D}_{\text{cruise}}$	lift to drag ratio in cruise flight	[-]
m_{htp}	mass horizontal stabilizer	[kg]
m_{pylon}	mass engine pylon	[kg]
m_{sys}	mass for electrical system and avionics	[kg]
m_{fur}	mass interior fittings (cargo floor etc.)	[kg]
m_{vtp}	mass vertical stabilizer	[kg]

$MTOW$	maximum take off weight	[kg]
W_{module}	module width	[m]
L_{HT}	momentum arm horizontal tail	[m]
L_{VT}	momentum arm vertical tail	[m]
n_{attack}	number of attacks	[-]
$N_{rotorblades}$	number of rotor blades	[-]
n_{rotor}	number of rotors VTOL	[-]
N_{rotor}	number of rotors cruise flight	[-]
n_{ppt}	number of turbines	[-]
H_{OL}	operational level	[m]
m_{op}	operational mass	[kg]
n_{PAX}	number of passengers	[-]
$P_{drag,aircraft}$	power to compensate drag, aircraft	[MW]
$P_{drag,rotor}$	power to compensate drag, rotor	[MW]
P_{pump}	pump power	[kW]
m_{pump}	pump weight	[kg]
R_oC_{to}	rate of climb take off	$[\frac{m}{s}]$
R_oC_{vcl}	rate of vertical climb take off	$[\frac{m}{s}]$
R_oD	rate of descent	$[\frac{m}{s}]$
R_oD_{ld}	rate of descent landing	$[\frac{m}{s}]$
A	rotor area	[m ²]
c_{rotor}	rotor blade depth	[m]
$d_{rotor,VTOL}$	rotor diameter VTOL	[m]
$d_{rotor,FF}$	rotor diameter forward flight	[m]
H_{SL}	sea level	[m]
H_{SC}	service ceiling	[m]
R	specific gas constant	$[\frac{J}{kgK}]$
$m_{eng,spec}$	specific power density electric engine	$[\frac{kW}{kg}]$
v_{sl}	stalling velocity in landing	$[\frac{m}{s}]$
v_{sto}	stalling velocity in take off	$[\frac{m}{s}]$
$SLST$	statistical combined engine thrust	[N]
s_{start}	starting distance	[m]
E_{to}	take off energy	[kWh]
P_{to}	take off power	[MW]
t_{to}	take off time	[s]
T	temperature	[K]
$\frac{T}{C}$	thickness to chord ratio of wing profiles	[-]
t_{wf}	time between water reservoir and fire	[s]
t_{cruise}	time in cruise flight	[s]
t_{base}	time in cruise flight between base and fire	[s]
v_{tip}	tip velocity of rotor blades (for VTOL)	$[\frac{m}{s}]$
t_{trans}	transition time	[s]
P_{trans}	transition power	[MW]
$P_{trans,ch}$	transition power from cruise to hover flight	[MW]
$P_{trans,hc}$	transition power from hover to cruise flight	[MW]

v_{trans}	transition velocity	$[\frac{m}{s}]$
m_{turbine}	turbine weight	$[kg]$
P_{vd}	vertical descent power	$[MW]$
P_{ld}	vertical landing power	$[MW]$
c_{VT}	vertical tail volume coefficient	$[-]$
t_{fillup}	water fillup time	$[s]$
m_{water}	water weight	$[kg]$
W	width	$[mm]$
w_{fus}	width of fuselage	$[m]$
S_{wing}	wing area	$[m^2]$
l_{m}	wing depth	$[m]$
W_L	wing load	$[kPa]$
m_{wing}	wing mass	$[kg]$
\bar{C}_W	wing mean chord	$[m]$
b	wingspan	$[m]$

Greek

α	angle of attack	$[^\circ]$
Λ	aspect ratio	$[-]$
γ_{climb}	climbing angle	$[^\circ]$
ρ	density	$[\frac{kg}{m^3}]$
η_{turbine}	efficiency turbine	$[-]$
η_{climb}	propulsive efficiency climb	$[-]$
η_{cruise}	propulsive efficiency cruise	$[-]$
η_{em}	propulsive efficiency electric engine	$[-]$
η_{hover}	propulsive efficiency hovering	$[-]$
$\eta_{\text{prop,ff}}$	propulsive efficiency propellor forward flight	$[-]$
η_{trans}	propulsive efficiency transition	$[-]$
ρ_{engine}	specific energy density of engine	$[\frac{kW}{kg}]$
$\rho_{\text{generator}}$	specific energy density of generator	$[\frac{kW}{kg}]$
ρ_{kerosin}	specific energy density of kerosin	$[\frac{kWh}{kg}]$
ϕ	sweep	$[^\circ]$
λ	taper ratio	$[-]$
γ_{H}	temperature gradient	$[\frac{K}{m}]$
θ_{tilt}	tilt angle	$[^\circ]$
C_{D0}	zero drag coefficient	$[-]$
C_L	zero lift coefficient	$[-]$

List of Figures

4	power-energy diagramm	9
5	Systemarchitecture	11
6	CG location during flight mission	14
7	bottom view with sensors	18
8	Mission profile	22
9	Mission profile in detail	23
10	$C_{a_{max}}$, typical flap angles for different high-lift devices	vii
11	Dragestimation	vii
12	The sensitivity of cruise speed on the aerial firefighting effectiveness and cost. [43]	viii
13	The impact of design range on the aerial firefighting effectiveness and cost. [43]	viii
14	The impact of operational range on the aerial firefighting effectiveness and cost. [43]	ix
15	The impact of payload on the aerial firefighting effectiveness and cost. [43]	ix
16	The impact of response time on the aerial firefighting effectiveness and cost. [43]	x
17	Naca 4415	x
18	section view cargo module	xi
19	section view water module	xi

List of Tables

1	fulfillment of requirements	4
2	mission energy	9
3	major battery data	11
4	results of stabilizer sizing	14
5	aircraft and mission data	iii
6	constants	iv
7	equation results	v
8	mass aircraft components	vi

1 Introduction and Analysis of the status quo

Wildfires have been increasing in size and frequency in Europe and all over the world due to a surge of fire-conducive weather, a combination of extreme heat and drought, caused by climate change. In addition to damaging the wild flora and fauna in the region and contributing further climate change by releasing massive amounts of greenhouse gases, it causes high economic losses. The impact of forest fire in the EU between 2000 and 2017 amounts to about 3 billion euros per year (over 54 billion euros collectively) and is projected to increase to over 5 billion a year by 2070-2100 for certain countries [1]. This provides a significant financial incentive to develop a modern aerial firefighting system that is effective and financially reasonable as well as capable to replace current firefighting fleets.

The 2022 DLR Design Challenge is tailored around this problem. The main task is to design a system of firefighting aircraft, capable of dropping 11000 l of water in one fire attack. Taking off from a regional airport (2000 ft above MSL) on a hot day in Europe. In the given scenario the wildfire (1000 ft above MSL) is 75 NM distanced from the airport while the distance between the fire and the nearest water source (2000ft above MSL) is 15 NM. The minimum operational ceiling is 8000 ft above MSL. The goal is to transport as much water to the fire as possible in a 24 hour window.

To potentially replace and enhance current firefighting fleets in Europe, we have to analyze their weaknesses. For example, we can look at the fleet established in the wake of the rescEU program by the European Union. Presently, 12 firefighting airplanes and 1 firefighting helicopter are available for deployment when wildfires demand a joint European effort. There are many aspects of the status quo to look at. First and foremost, they are all manned aerial operations, putting human lives at risk, increasing operational costs, and limiting the operation time to an average of about 12 hours. Additionally, they are not equipped with the technology to efficiently release water since they just drop the water out of a tank. Furthermore, they lack high maneuverability and require a landing point, implying that they need to return to a base to refill their water and or fuel tank for the next fire attack. Looking at the financial side, the capital and operational costs are extremely high. A new fleet would have to be able to provide better characteristics in the mentioned fields. That is the aim of the presented concept.

2 Concept Summary

2.1 Concept Overview

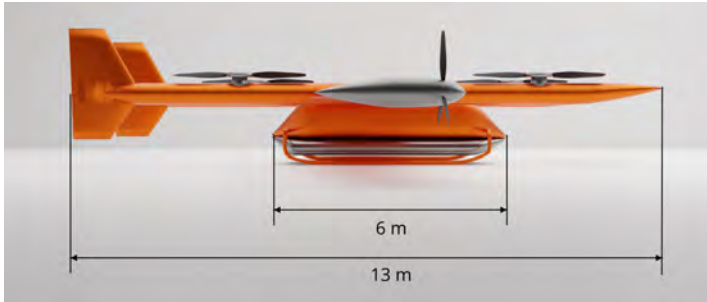


Figure 1: side view



Figure 2: front view

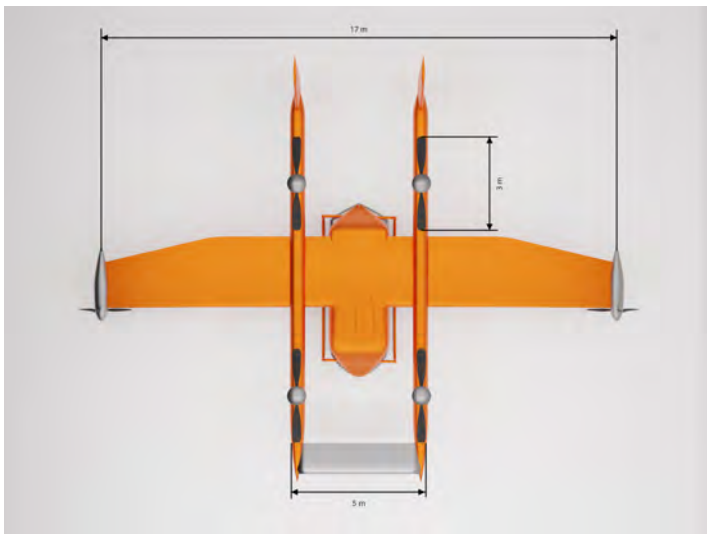


Figure 3: top view

Technical Data

MTOW	5679 kg
L_{aircraft}	13 m
S_{wing}	17 m
$d_{\text{rotor,VTOL}}$	3 m
$d_{\text{rotor,FF}}$	2 m
L_{module}	6 m
W_{module}	2 m
V_{water}	1100 l

2.2 Key Technologies

Hybrid electric propulsion. This technology together with light and powerful electric motors allows for VTOL capabilities without adding excessive weight or requiring complex swivel mechanisms. Wing tip propulsion. Reducing the induced drag in cruise flight, mounting the propellers for horizontal propulsion and the wing tips enhances efficiency and increases the range of the aircraft. Modular Design. Switching between configurations for off-season uses can be realized with ease by using modules instead of current retrofit technology. Furthermore, this concept offers new possibilities for rescue and transport missions during a fire attack. Sensor and software technology for autonomous flight. Eliminating risk to the pilot's life while reducing operational costs autonomous flight is used as an important key technology. Additionally this system includes the flight stability system providing reliance against gusts and higher flight stability for the canard configuration. Lithium sulfur batteries have a much higher specific energy density and are less susceptible to fire, in case of cell malfunction. Carbon fiber composites ensure the lowest structural weight possible as well as favorable corrosion characteristics.

2.3 Evaluation

2.3.1 Safety and Failure Modes

Aerial firefighting comes with a lot of risks due to dangerous wind conditions, a shifting Cg, limited visibility, and multitasking of the pilots leading to human errors. To eliminate the danger to these people the PEL-E-FAN-T is operated remotely and only needs to be manually controlled in critical flight phases, flying autonomously in redundant and predictable situations such as cruise flight, therefore reducing the workload on the pilot. The risk for failure of the required computer systems is negligible due to redundancy. Though a software-based issue can occur, not being able to find a solution to a given problem, and has to be accounted for. In this case, the system switches to remote control to let the pilot handle the situation. In case of the failure of one rotor in a VTOL flight phase the aircraft is capable to stabilize itself using a combination of internal and external sensors [2]. Should a rotor fail in cruise flight then the other horizontal motor is turned off and a combination of gliding and VTOL capabilities are used to land safely. Although capable of withstanding gusty winds, extreme situations have to be accounted for. Therefore the PEL-E-FAN-T can switch into VTOL mode if stall of flight instability occurs. Should communication with the aircraft not be possible then the aircraft will transition itself into hover mode and find one of the safe locations to land, defined before and updated during the fire attack.

2.3.2 Fulfillment of Requirements

Table 1: fulfillment of requirements

Number	PEL-E-FAN-T fleet	achievement
1	mtow not greater than 5670 kg	limit achieved
2	can operate at a service ceiling of 8000 ft	threshold achieved
3	ability to transport 11000 l in one fireattack	goal achieved
4	minimized noise at take off	goal achieved
5	VSTOL capabilities	goal achieved
6	ability to take in water from small watersources (currently only achieved by helicopters)	goal achieved
7	operated remotely or by only one pilot	goal achieved
8	automatic gust and wind correction for precise water-drop	goal achieved
9	operation at night and under low visibility	goal achieved
10	24 h operationable	goal achieved

3 Design Overview

"PEL-E-FAN-T" is designed for fire fighting in the safest and best way possible. As a fixed-wing VTOL vehicle, it combines vertical take-off and landing capabilities, necessary for a water intake from small water sources only approachable by helicopters, with horizontal speed and efficiency offered by traditional airplanes. Maximizing reliability and minimizing possible damage by in-flight failures, the concept uses fixed rotors instead of tilt rotors, which have proven to be unreliable in the proximity of water, especially salt water. Maneuverability is enhanced by using a canard layout. Combining existing and well-proven technologies the "PEL-E-FAN-T" operates as a UAV minimizing the risk to human life, minimizing operational costs, and being capable to fight fires 24h a day. The efficiency of the fire attacks is further increased by using a fleet consisting of 10 modular aircraft, having the ability to coordinate in a swarm autonomously while the pilot only has to maneuver critical flight phases such as water drop or water intake. The "PEL-E-FAN-T" is designed to change Modules rapidly compared to Retrofit techniques, which minimizes costs and cuts conversion time massively for the off-season use as a cargo drone. By changing Modules one to two hours a fast and tailored response to the fire with a heterogeneous fleet is possible.

3.1 Aircraft Design

"PEL-E-FAN-T" is designed for fire fighting in the safest and most efficient way possible. As a fixed-wing VTOL vehicle, it combines vertical take-off and landing capabilities, necessary for a water intake from small water sources only approachable by helicopters, with horizontal speed and efficiency offered by traditional airplanes. Maximizing reliability and minimizing possible damage by in-flight failures, the concept uses fixed rotors instead of tilt rotors, which have proven to be unreliable in the proximity of water, especially salt water. Furthermore, tilt rotors are not considered due to their high technical complexity, size and their weight penalty caused by the the tilt and variable pitch mechanisms [3]. Exploiting the high specific power of electric motors, they can be mounted inside longitudinal struts in a symmetric manner in relation to the center of gravity resulting in stable vertical flight. Looking at possible arrangements of the propulsion on hybrid-electric aircraft, distributed electric propulsion (DEP) and wing tip propulsion are discussed most often [4]. DEP uses small propellers mounted along the leading edge of the wing, increasing the lift coefficient at low speeds making it possible to reduce the wing size [5] [6]. By using many sources of thrust this concept is very resilient to failure. However, DEP can cause a significant increase in the operational empty weight and increases the complexity of the aircraft considerably [5]. Wing tip propulsion is capable of reducing drag by attenuating the wing tip vortex due to the propeller rotating counter the vortex [7]. This results in a reduction of induced drag and therefore higher cruise efficiency. Considering these advantages and drawbacks the propellers for horizontal flight are mounted on the wing tips of the aircraft.

The horizontal stabilizer is mounted between the struts far away from the fuselage reducing induced drag and improving flight stability as well as controll by maximizing the lever of the controll surface. The canard configuration further improves maneuverability and the stall behavior of the aircraft. Electric motors are used because of their high specific power, making it possible to place them into the longitudinal struts next to the fuselage as well as on the wing tips. Combining existing and well-proven technologies the "PEL-E-FAN-T" operates as a UAV minimizing the risk to human life, minimizing operational costs, and being capable of fighting fires 24h a day. The efficiency of the fire attacks is further increased by using a fleet consisting of 10 modular aircraft, having the ability to coordinate in a swarm autonomously while the pilot only has to maneuver critical flight phases such as water drop or water intake. The "PEL-E-FAN-T" is designed to change Modules rapidly compared to Retrofit techniques, which minimizes costs and cuts conversion time massively for off-season use as a cargo drone. By changing Modules one to two hours a fast and tailored response to the fire with a heterogeneous fleet is possible.

3.2 Hybrid-electric Powertrain

The main drivers behind design decisions regarding the propulsion system of PEL-E-FAN-T were the maximisation of useful load and minimisation of weight. Reducing both environmental and noise pollution was also desired. Optimising for a greater useful load allowed us to fulfil the mission requirements with a smaller fleet size. This has a major impact on costs and therefore the economic feasibility of the project. Considering the requirements regarding emissions, minimum range and the flight profile, it was determined that these can only be met with the use of hybrid propulsion systems. The electric motors are both relatively light and cheap. They furthermore allow them to be placed as structural components within the airframe, saving both weight and money [8]. Additionally, all-electric motors can be controlled individually, which allows for stable hovering, while taking in water. Hydrogen propulsion was considered but ultimately discarded, because of a lack of hydrogen infrastructure. Exemplary

for the low hydrogen coverage, Spain can be used. It only has 120 hydrogen fuel stations, which is insufficient for use in quick emergency service vehicles [9]. That's the reason why the PEL-E-FAN-T is based on a hybrid propulsion system with conventional turbines. This suits the mission profile perfectly. Airbus and Siemens predict that by 2030 it is possible to build passenger aircraft with a capacity of fewer than 100 seats with hybrid propulsion [10]. This shows the potential of hybrid propulsion and the feasibility of operating a hybrid aircraft with our MTOW at EIS. Furthermore, simulations of hybrid-electric propulsion systems suggest that by the EIS of PEL-E-FAN-T, the specific energy density of batteries will be high enough to complete short-haul missions. Since modern aircraft can be expected to have a service life of 30-35 years, hybrid-electric propulsion systems can significantly reduce emissions compared to conventionally powered aircraft [11]. On top of the aforementioned advantages, further reduction of aircraft noise can be achieved through hybrid-electric propulsion. Components that generate the most noise can be positioned in more soundproofed areas. Furthermore, it is possible to reduce the propeller noise by operating at lower rotational speeds by using the high torque of the electric motor [8].

Concerning the technological readiness level, the technology of PEL-E-FAN-T is based on a wide variety of concepts that already exist or are currently under development. Examples for the general configuration are the "ALIA-250c" from Beta Technologies and the "Chaparral" from Elroy Air. In addition, there are various other concepts with electric and hybrid drives, which have a proven TRL between 5 and 7. Examples with this TRL include "E-Fan X" which is being designed in collaboration between Airbus, Rolls Royce and Siemens and the 9 Passenger aircraft "Alice" engineered by EVIATION [12]. These examples show a wide range of functional deployment options, which are all in agreement with the given entry into service. This allows us to justify the feasibility of our configuration with a hybrid propulsion system.

3.2.1 Mechanical link

In this configuration, only the electric motors are connected to the propellers. The turbine engine drive generators, which then drive the motors or charge the batteries through a rectifier. During times of low power demand (e.g. cruise flight), the batteries can be recharged, which significantly improves the total range. The simplicity of this system allows for easy propulsion control, which enables the pilot to concentrate on his essential tasks during the firefighting attack. Furthermore, the turbine engine can run constantly at its best operating power and speed [12]. Another advantage of the PEL-E-FAN-T's drive system is that the series hybrid architecture allows a multiple rotor layout, where each propeller has its electric motor [13]. This makes it possible to place the rotors optimally and at the same time, it improves stability during the water intake and flight, because each motor is individually controllable. This allows the pilot to be more responsive to environmental conditions [12].

3.2.2 Power and Energy demand

To estimate the power demand of the aircraft, the air density and aircraft data had to be determined, this is done in other chapters of this paper, and all values and parameters can be found in the appendix. Using the equations 1 to 24 from the paper [14], the power and energy demand will be determined below.

First of all, the power to hover P_{hover} the Aircraft was calculated since it is a critical flight maneuver. The Pump that is used to fill up the aircraft's water tank, in this segment of the flight, has an approximate power of 5 kW and only needs about 20 s to pump up the 1100 kg of water. This power is very small, less than 0.5 %, in comparison to the power that is needed

to hover the aircraft. For these calculations the pump's power and the energy consumption are negligible.

$$P_{hover} = \frac{W_0}{\eta_{hover}} \cdot \sqrt{\frac{DL}{2 \cdot \rho}} \quad (1)$$

The takeoff power P_{to} is calculated by using P_{hover} and depends on the Rate of climb R_{oCto} and the hover velocity v_h , which is calculated using (3).

$$P_{to} = P_{hover} \cdot \left[\frac{R_{oCto}}{2 \cdot v_h} + \sqrt{\left(\frac{R_{oCto}}{2 \cdot v_h}\right)^2 + 1} \right] \quad (2)$$

After takeoff or starting from hovering the aircraft vertically climbs to the desired height for the transition to take place and does this with R_{oCvcl} . Besides that, the same values as in (4) are being used for this calculations.

$$P_{vcl} = P_{hover} \cdot \left[\frac{R_{oCvcl}}{2 \cdot v_h} + \sqrt{\left(\frac{R_{oCvcl}}{2 \cdot v_h}\right)^2 + 1} \right] \quad (3)$$

Now that the aircraft has reached its desired height and the transition starts. Using the forward propellers the aircraft starts to gain horizontal velocity, but still needs its VTOL motors to produce enough lift that the aircraft does not lose altitude. The required power is the sum of the induced power $P_{induced}$, the power to overcome the drag of the rotor blades $P_{drag,rotor}$ and the power to overcome the drag of the aircraft. To calculate these powers the transition velocity v_{trans} was set and the blade solidity σ was calculated, as well as the speed at the rotor tips v_{tip} . The other terms and coefficients can be found in "Table 5".

$$P_{trans,hc} = P_{induced} + P_{drag,rotor} + P_{drag,aircraft} \quad (4)$$

The Aircraft has now reached the transition velocity and goes into the climbing flight. It is estimated that the rate of climb R_{oCcl} is constant and can be calculated by the climb angle γ_{climb} and the climbing speed v_{climb} [14]. With this, the power for the climbing flight can be calculated using (13).

$$P_{climb} = \frac{W_0}{\eta_{climb}} \cdot \left(R_{oCcl} + \frac{v_{climb}}{L_{D,climb}} \right) \quad (5)$$

Following the climb, the aircraft accelerates to cruise speed v_{cruise} and starts its cruise flight, to simplify the calculations all segments of the flight were seen as continuous. The lift to drag ratio $\frac{L}{D}_{cruise}$ and the efficiency coefficient η_{cruise} [14] can be found in "Table 5". As a simplification the power for the descent flight is included in this equation [14].

$$P_{cruise} = \frac{W_0 \cdot v_{cruise}}{L_{D,cruise} \cdot \eta_{cruise}} \quad (6)$$

As the aircraft prepares for landing or goes into the hovering state, a second transition takes place. The calculations for that are similar to the ones for the first transition(11) [14]. The velocity of the second transition was set to be equal to the velocity of the first.

$$P_{trans,ch} = \frac{W_0}{\eta_{trans}} \cdot \sqrt{\frac{-(v_{trans}^2)}{2} + \sqrt{\left(\frac{v_{trans}^2}{2}\right)^2 + \left(\frac{W_0}{2 \cdot \rho \cdot A \cdot n_{rotor}}\right)^2} + \dots}$$

$$\rho \cdot A \cdot v_{tip}^3 \cdot \left(\frac{\sigma \cdot C_{D,rotor}}{8} \right) + 0,5 \cdot \rho \cdot v_{trans}^3 \cdot C_{D,trans} \cdot S_{wing} \quad (7)$$

Coming to a full stop in midair, the aircraft starts to descend. Here again, already known equations can be used. The calculation of the descending Power is the same as the ones for the vertical climb. Instead of R_{oC} , the rate of descent R_{oD} is used, and caused by the downwards movement, is negative. If the value of R_{oD} is between -2 and 0 the airflow is in a vortex stream state, here the flow is turbulent [15]. An approximation for the induced velocity $v_{i,descent}$ can then be made with (8) going back to an experimental approach by [16].

$$v_{i,desc} = v_h \cdot \left[k + k_1 \cdot \left(\frac{R_{oD}}{v_h} \right) + k_2 \cdot \left(\frac{R_{oD}}{v_h} \right)^2 + k_3 \cdot \left(\frac{R_{oD}}{v_h} \right)^3 + k_4 \cdot \left(\frac{R_{oD}}{v_h} \right)^4 \right] \quad (8)$$

$$P_{vd} = P_{hover} \cdot \left[\frac{R_{oD}}{v_h} + \left(\frac{v_{i,desc}}{v_h} \right) \right] \quad (9)$$

As the aircraft finishes its mission it sets land. The landing power can be calculated using (16) and (17) but instead of R_{oD} , R_{oDld} is applied.

$$P_{ld} = P_{hover} \cdot \left[\frac{R_{oDld}}{v_h} + \left(\frac{v_{i,ld}}{v_h} \right) \right] \quad (10)$$

To simplify the calculations, the MTOW was used as the weight of the aircraft in every stage of the flight. The lift and drag coefficients as well as any other term that is not specifically calculated above can be found in “Table 4”.

With the calculated powers an approximation for the mass of the motor can be made. Assuming the specific power-to-weight ratio is $10 \frac{kW}{kg}$, like the Equipemake Ampere-220 [17], the installed electric motor mass m_{eng} can be calculated. For that, it is necessary to use the highest required power, P_{vcl} , and the efficiency of the motors of about 95% [18].

$$m_{eng,vtol} = \frac{P_{vcl}}{m_{eng,spec} \cdot \eta_{em}} \quad (11)$$

The same method can be applied to estimate the mass of the motors that propel the aircraft forward. The segment with the maximum required power is the climbing flight with P_{climb} . The power that is demanded to have a R_{oCsc} at the service ceiling can be calculated with the following equation and can be managed with the installed power, where v_{climb} will be generated with a γ_{climb} of 8 ° instead of 4°.

$$v_{climb} = \frac{R_{oCcl}}{\sin(\gamma_{climb})} \quad (12)$$

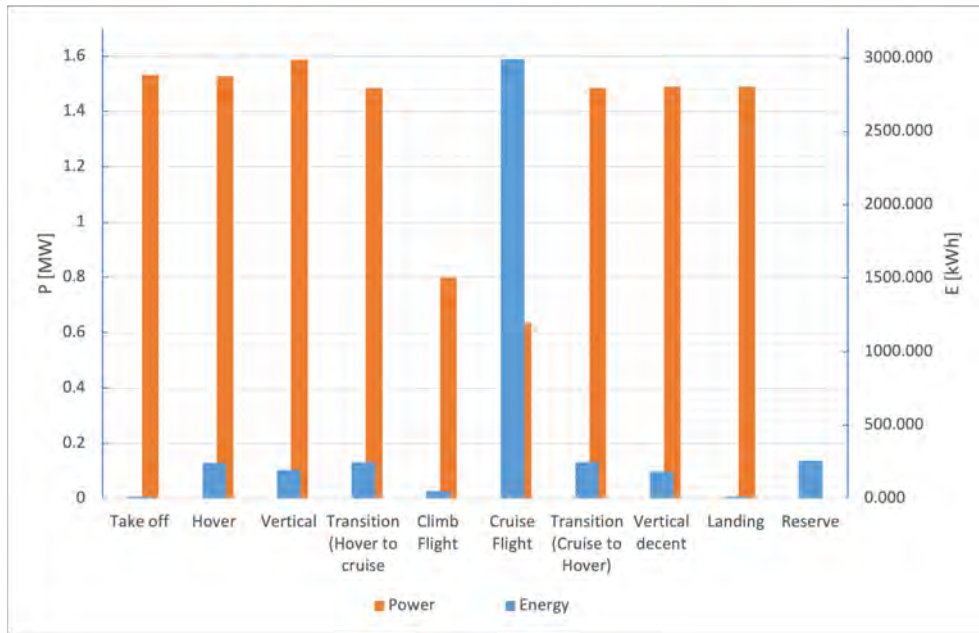
$$P_{climb,sc} = \frac{W_0}{\eta_{climb}} \cdot \left(R_{oCcl} + \frac{v_{climb}}{L_{D,climb}} \right) \quad (13)$$

To provide this energy two turbogenerators like the PT6C-67 C were installed. They have a continuous output of 815 kW and takeoff power of 861 kW [19]. In some segments of the flight, this power is not enough and the difference will be provided by the battery. In case one engine fails, the other turbine can produce a total power of up to 1217 kW for 2 $\frac{1}{2}$ minutes, and a continuous output of 1064 kW together with the battery it has enough power to fly the aircraft to the nearest airport.

Now that the power for each maneuver is determined, the energy demand can be estimated. First, it is necessary to calculate the time the aircraft spends in each segment, by using the velocities and distances [14]. To calculate the total energy demand the number of firefighting attacks was iteratively defined. Each aircraft fulfills 20 attacks and 19 water intakes. The

Table 2: mission energy

	TO	HO	VC	The	CIF	CrF	Tch	VD	L	R	TE
$t_{\text{total}}[\text{s}]$	30	570	444	600	222	16960	600	444	30	-	19870
P [kW]	1533	1527	1587	1485	800	635	1485	1490	1489	-	-
E [kWh]	12.8	241.7	195.8	247.0	49.4	2991.0	247.0	184.0	12.4	305.4	4487.7

**Figure 4:** power-energy diagramm

following equation was used to calculate the individual and the total energy demand.

$$E = P \cdot t \quad (14)$$

The amount of fuel that is needed for this operation is estimated by using the energy density of kerosine and the efficiency of the turbine, which is set to 40% considering the entry into the service year and the fact that future turbines and generators will be optimized for each other. An example of that is the new Turbogenerator from Rolls Royce [20], a turbine specified to supply electric aircraft with power. This leads to an approximate fuel mass of 933 kg kerosine for 20 attacks. In this mass is a reserve included, enough for a flight of 75 NM and the safe landing of the aircraft.

3.2.3 Comparison with conventional firefighting aircraft

One of the huge advantages of the “PEL-E-FAN-T” is its ability to take off and land vertically as well as hover in the air which is a very useful skill for taking in water at small reservoirs. This distinguishes it from normal airplanes who need rollways and long open lakes or rivers to fill up on water. A helicopter can target small and narrow water reservoirs. Still, it lacks the ability to efficiently cruise on long flights, which the “PEL-E-FAN-T” is capable of. For instance, the Bell 212 can carry an amount of 1360 liters of water at once [21] and has a range

of 700 km and a cruise speed of 186 km/h [22]. The water capacity of the “PEL-E-FAN-T” is, 1100kg, a bit less but it has a range of 1389 km and a cruise speed of $270 \frac{km}{h}$, in this scenario. These abilities give the “PEL-E-FAN-T” a higher efficiency, both on full consumption and on water drops per hour.

3.2.4 Battery and system architecture

“PEL-E-FAN-T” is designed around a hybrid system consisting of two turbine engines, each powering an electrical generator. The turbo generators supply the bulk of electrical power needed during a mission to the electric motors. The Battery system of “PEL-E-FAN-T” is not designed to act as the sole energy source for the entire flight mission. Instead, it acts as an energy buffer in situations where the demand cannot be satisfied by the turbo generators alone, like during water intake. It, furthermore, stores enough energy to vacate the danger zone and reach a landing spot within a 15 km radius in case of complete turbine or generator failure.

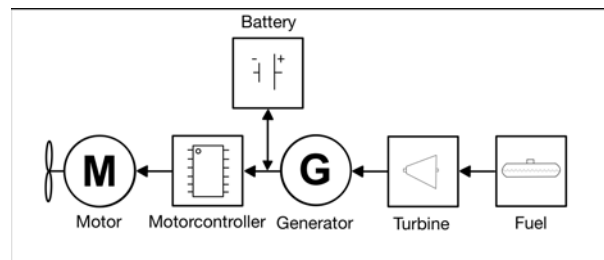
The following battery characteristics were mainly considered during the design phase:

1. high battery safety
2. high specific energy density
3. sufficient avg. discharge rate (C-Rate)
4. high cycle life/ longevity
5. low cost
6. environmental impact

Lithium-Sulfur Batteries, although not in serial production yet, look most auspicious. They are far superior in terms of safety compared to conventional lithium-ion batteries because their cell chemistry and operating mechanism greatly decrease the risk of catastrophic cell failure. [23] While a thermal runaway event as in Li-Ion cells remains possible, depending on the electrolyte used, the extent of such events is far lower, according to research [23]. The specific energy density of Li-S Batteries is said to increase to 650 Wh/kg by 2030 [24], while the cost is forecasted to be substantially lower than Li-Ion batteries due to much lower material and logistical costs due to their cell stability [25]. The abundance of Sulfur across all areas of the world and its intoxic nature position Li-S cells as an environmentally favorable battery option [26]. Disadvantageous properties of the Li-S battery are their relatively low longevity and low average discharge Rate. The cycle life is said to increase to 1000-2500 cycles until the cell falls short of 80 % of the design capacity [24]. “PEL-E-FAN-T” is designed with a specific energy density of 400 Wh/kg in mind. Unfortunately, new Battery systems pushing the boundaries of what is possible regarding energy density are usually poor performers in terms of longevity, C-Rating and reliability. Since the battery system ought to be dependable for many consecutive missions, we chose to take a conservative estimate for battery performance. With this conservative approach, we can ensure that our design is not compromised due to slow battery development.

Table 3: major battery data

Data	Unit	Value
Gravimetric energy density	$[\frac{Wh}{kg}]$	400
Volumetric energy density	$[\frac{Wh}{l}]$	300
Total energy	[kWh]	77.6
Weight	[kg]	194
Volume	$[m^3]$	0.259

**Figure 5:** Systemarchitecture

3.3 Modules

One of the key features of the “PEL-E-FAN-T” is the modular design. The mechanism to change Modules is simple and fast to minimize time spent on the ground. All Modules and aircraft have to be equipped with sensors for lining up with the aircraft. A mechanical linking system consisting of a crane in the main aircraft to lift the modules into place as well as fixing points where the modules are safely locked into place. Because those parts can get exposed to sea water, they consist of stainless steel. Additionally, an electrical connection has to be provided for certain modules. To Change modules, the aircraft is positioned in a place where the module can be stored, via ground handling wheels (similar to those for helicopters). The module is mechanically released and let down by the crane. Then the “PEL-E-FAN-T” is manually positioned above the desired module, being lined up via sensor feedback. After picking up the module, locking it into place, and potentially manually linking their electronics the aircraft is again ready for take-off. Designing such a system in detail should not prove to be very difficult since companies such as Elroy Air have already implemented similar systems on their cargo drones. In case of switching to a module with different dimensions, the “PEL-E-FAN-T” gets jacked up with standardized helicopter lifting jacks at four points on the longitudinal braces to change the skids so the next module will fit beneath the aircraft. To reduce weight and increase efficiency all modules consist of CFRP.

3.3.1 Firefighting Configuration

The most critical module to fulfill the task the “PEL-E-FAN-T” was designed for are the firefighting modules. To minimize flight instabilities from pendulum effects which are difficult to control in a UAV the firefighting module is equipped with a belly tank with a volume of 1100l. To avoid carrying empty mass around, the fire fighting module got smaller dimensions. With a width of 1.5, a height of 0.5 and a length of 6 meters it is the smallest among all of them. Covering small and big water sources the module has to be able to function without

complications. To take in water as fast as possible from small to large water sources, a hose (diameter 6 inches) with a hover refill pump (450 hp) can be installed, capable of pumping 1500 Gallons per minute (5678.118 l/min) and only weighing in at 100 lbs (45.36kg). These figures are derived from current models by KAWAK AVIATION TECHNOLOGIES. The tank fills up in only 20 seconds. At large accumulations of water (lakes, the sea etc.) scooping is a more efficient way to fill up the water tank. It is within reasonable possibility that a “Sea Snorkel” like the one on the S-64 Helitanker can be installed and used to extend the range of the aircraft since hovering is not necessary. The “Sea Snorkel” could replace the traditional snorkel in suitable circumstances, making it necessary for the module to have a mechanism to easily replace one system with the other. In case of using a fire retardant an additional tank can be implemented into the module for storage. An additional pump will be necessary for rationing the needed volume of chemicals to ensure the perfect mixture of water and fire retardant when dropped onto the fire, which will be provided with the needed electricity through high current cables.

3.3.2 Cargo Configuration

Similar to the system Elroy air is already using, the “PEL-E-FAN-T” can function as a cargo drone both in the firefighting season and the off season. With its modular design capability, the aircraft is designed to minimize loading time, maximizing efficiency and income. Additionally, it eliminates piloting costs since the transport of cargo happens fully autonomously, since there are no critical maneuvers (like in the firefighting mission) where a pilot would be needed. The Cargo feature can not only be used in transporting goods between cities but also to haul items to remote areas where infrastructure might be lacking or the access is limited, since the “PEL-E-FAN-T” has VTOL capabilities and only needs a small area to land. The Cargo module has an aerodynamically improved shape while being flat at the bottom to stand stable on the ground. With a height and width of 2 meters and a length of 6 meters it is designed to fit an LD2 container into it, making transshipment of bigger machinery possible. For loading and unloading the Cargo, a hatch with a width of 1,80 and height of 1,72 meters is located on each side of the module.

3.3.3 Evacuation Configuration

Besides the firefighting module being the primarily used configuration during the whole operation, an evacuation module can also be necessary if a person has to be rescued. Therefore, the cargo module can be modified within one to two hours making space for a rescue stretcher, devices for respiratory monitoring, an emergency backpack and a seat for a paramedic. To run all the included devices, the module will be provided with the needed electricity through power cables.

3.3.4 Passenger Configuration

During off season the “PEL-E-FAN-T” can be used in the Urban Air Mobility sector in the passenger configuration. Therefore, a similar module to the cargo with the same dimensions will be used, saving development time. It offers room for up to six passengers and has windows on each side of the cell. The hatch will also be similar to the one used at the cargo module. All the included electrical devices like the lights and the air conditioning will be provided with the needed electricity through high current cables.

3.4 Aerodynamics

One of the most important aspects of the "PEL-E-FAN-T" is its unconventional aerodynamic layout.

3.4.1 Wing

The wing geometry is tailored around the requirements for the aircraft. Flying at subsonic speeds, sweeping the wing is not necessary. Increasing aerodynamic efficiency the outer sections are tapered providing a reduction in induced drag in comparison to an untapered wing and saving manufacturing costs compared to an elliptical wing. As the Profile of the Wing NACA 4415 has been chosen, providing enough lift in cruise flight to fly with an angle of attack near zero degrees as well as a low sensitivity to different Reynolds numbers in the operating window of the PEL-E-FAN-T as seen in figure 17. To further reduce the stalling speeds triple slotted flaps are installed making it possible to reach a local C_L of 3.5 with a deflection angle of about 40° (figure 10 from [27]). This reliable and proven technology enables the PEL-E-FAN-T to reach a low speed of $129.8 \frac{km}{h}$. For flight situations where a lower speed is required, the VTOL capabilities of the PEL-E-FAN-T are used.

3.4.2 Canard and vertical stabilizer

During a fire attack the aircraft has to deal with several external influences, such as wind gusts, that can change the flight behavior and therefore the precise fire suppression. The aircraft also has to carry a huge volume of water or chemicals to the source of the fire, which requires a lot of lifting force. The canard configuration of the aircraft provides several advantages that are useful in terms of this demand profile. Its two main purposes are firstly to improve the maneuverability of the aircraft, which is essential in slow flight conditions and secondly to reduce wing loading of the main wing in critical flight situations. Especially the improved maneuverability is essential for the remote control in flight phases such as the water drop since the pilot cannot judge critical flight situations as well as he could if he physically sat inside the aircraft. To benefit from the anti stall characteristics of this configuration the canard has to stall before the main wing avoiding the loss of lift. Benefiting from modern control technology the PEL-E-FAN-T avoids flight stability disadvantages often associated with the canard configuration, allowing the use of relaxed static stability without compromising handling qualities [28]. Sizing the canard, the approximation method for horizontal stabilizers by RAYMER is used (formula 25). Instead of using a tail volume coefficient of 0.1 for the canard described by RAYMER, a more conservative estimation of 0.29 has been chosen to account for possible modifications in further development aiding flight stability. The canard position has to be above or below the main wing and far away from the main wing to reduce the manipulation of the flow around the main wing [29] and at the same time maximizing the moment arm. Therefore the canard is mounted on the highest point most forward of the struts while the main wing is positioned on the lowest possible point. Mounting it in between the struts also comes with the benefit of a reduction in induced drag as well as less influence of the canard vortex on the main wing. The vertical stabilizer has been positioned at the farthest point aft the main wing to maximize the momentum arm, minimizing its wing area. The sizing follows the approach by RAYMER (formula 26). The results of the sizing of the vertical as well as the horizontal stabilizer can be seen in table 1.

Table 4: results of stabilizer sizing

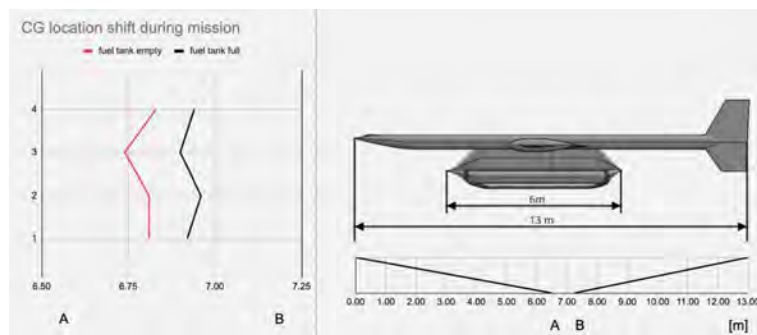
	Moment Arm [m]	Area [m^2]
Canard	6	4.002
Horizontal Stabilizer	7	5.508

3.4.3 Drag estimation

To estimate the zero-lift drag coefficient C_{D0} of the aircraft, OpenVSP software with a simplified model was used. The firefighting configuration has been used for this estimation. Table A 1 shows the drag contribution of each surface. Depiction Figure 11 shows the resulting distribution of pressures over the body of the PEL-E-FAN-T.

3.5 Shifting CG

Dealing with shifts in Cg location is of utmost importance for all firefighting aircraft, as during water intake and fire attacks, changes occur rapidly, and water usually slushes during flight. "PEL-E-FAN-T", with its canard configuration and multirotor design, is excellently equipped to cope with all these problems. The canard configuration allows for a wider CG range than standard configuration aircraft. Furthermore, to prevent both fuel and water from slushing and endangering the stability of the aircraft, both tanks are compartmentalized. All four vertical engines can be controlled individually. This not only enables VTOL capabilities in the first place but also provides a unique coping mechanism for residual slushing. During water drop, the aircraft can be retrimmed quickly thanks to the canards. The canards are sized larger than necessary for standard aircraft to provide additional maneuverability. The shift in CG-location over an entire mission is shown in figure 6.

**Figure 6:** CG location during flight mission

3.6 Mass

A first accurate analysis of an aircraft's mass is vital for all further design work. The method applied to obtain the desired approximate mass originates from F. Dorbath, initially published in the Aeronautical Engineering Handbook. In contrast to other methods, Dorbath makes do with less information and was found to yield results similar to or even more accurate than different approaches, all while consistently staying on the conservative side. [30] Furthermore,

it allows for a rectangular fuselage and includes optimized formulas for aircraft below 5700kg MTOW. Dorbath is, therefore, best suited for our application. The method divides the aircraft into ten subgroups and approximates the weight of all relevant systems and structures within each group: Wing Mass, Fuselage Mass, Horizontal Tail Plane Mass, Vertical Tail Plane Mass, Landing Gear Mass, Pylon Mass, Power Units Mass, Systems Mass, Operators Items Mass. The unique shape of the fuselage, with its twin-boom design and central fuselage box, posed a unique challenge during weight analysis. It was solved by adding the volume of the booms to the rectangular fuselage box and calculating the m_{fus} with the resulting increased length. Other approaches like calculating m_{fus} for all three fuselage components separately would have resulted in unacceptable deviations since, as stated previously, formula m_{fus} not only includes the hull structure but all relevant subsystems and structures within the fuselage. These include the cargo hold floor, Paneling, and special structures like a landing gear bay. These subsystems are already accounted for twice due to the separately analyzed module hull structures, and some, like the landing gear bay structure, are not part of "PEL-E-FAN-T". The non-conservative approach to approximating the twin-boom fuselage weight is thereby accounted for. Since "PEL-E-FAN-T" uses simple skids instead of conventional landing gear, the calculated value for the landing gear was halved. Correction factors for the use of composite structures got applied to the wing and fuselage masses.

4 Avionics and Autonomy

A large percentage of the operating costs of a small aircraft are personal expenses [31]. For many years the number of people operating an aircraft shrunk, whereas the number of electronic assistance systems increased. In the following, two ways of further decreasing the crew costs are described.

4.1 Single Pilot Operation

The first concept is the SPO with only the captain in the aircraft some of the tasks previously done by the Co-Pilot are now carried out by AS and the GO. But still, the PIC has the final decision-making power over the aircraft and delegates tasks to the AS and the ground operator [31]. In the SPO the operating conditions can be divided into four categories, or as it is described in, [31] TC. For that two criteria are important, the pilot condition, either normal or incapacitated, and the flight condition, which is nominal or off-nominal. TC1 is the average operating state and means the pilot's condition is normal and the flight condition is nominal. When the flight conditions change to off-nominal the operating conditions switch to TC2. Is the pilot incapacitated, meaning he is not able to control the aircraft for example caused by a health issue, and the flight conditions are nominal the operating state is set to TC3. The worst-case scenario would be TC4 where the pilot is incapacitated and the flight conditions are off-nominal. A Dispatcher works in the AOC, where the air traffic is controlled and managed, in the case of an SPO he turns into a GO, the co-pilot on the ground [31]. Supporting the PIC he helps plan the route, checking the list before takeoff, and provides him with information about the air traffic and possible changes in the weather conditions or the mission profile. In TC1 scenarios one GO can work together with up to 20 pilots in different aircraft [31]. But if it comes to an abnormal situation the conditions change to TC2 or higher. In this case, a very high workload must be managed by the pilot, and one-to-one support is needed. In TC3 or 4 a GO takes over the control of the aircraft, which means he must have the possibilities and capabilities to fly this aircraft. Therefore the GO must be an active pilot and the AOC must have the technical abilities and instruments to radio control an aircraft, it has to be equipped with a second cockpit. To realize the SPO there are two concepts. First of all the hybrid ground operator unit, where one GO is responsible for all tasks, from dispatching to radio-controlled flying of the aircraft, and the special ground unit, where the GO supports the aircraft until, in case of a TC3 or 4, a ground pilot has to step in. One advantage of the SPO is the fact that there is always a pilot on board the aircraft. This leads to better situational awareness and shorter responding times. However, this is also its greatest disadvantage. Since in firefighting scenarios dangerous maneuvers are performed and so human lives are put at risk. But still, one safety factor is the fact that SPO aircraft can fly partially autonomous and can be remote-controlled. In the end this concept only leads to little savings in the personal sector and having a pilot on board means having a Cockpit, which costs space and mass, limited resources in aviation.

4.2 Autonomous Flight

An UAS is marked by the fact that there is no operating pilot needed in the air. A part of UAS is an UAV. This UAV can be either remote-controlled or fly autonomously. Many Nations have been using UAVs for many years now, for instance, the MQ9-A „Reaper“ or the RQ-4B „Global Hawk“. Also, Amazon put their first packaging drones to the test [32] and in September 2021 one of the first firefighting UAVs was introduced, the “WILD-HOPPER” [33].

4.2.1 Hardware

To realize a UAS a series of sensors, that can perform in any weather or light condition, are needed. As well as the “WILD-HOPPER“, “PEL-E-FAN-T“ has two independent navigation systems. On one side it uses Galileo, the European satellite navigation system, which is the most accurate in the world, with a precision of 10-50 cm [34], and on the other side, an IMU is used. In case Galileo should fail, GPS steps into work. An IMU consists of acceleration sensors, gyroscopes and magnetometers. Using acceleration and rotation data of the aircraft, position and velocity can be calculated. The magnetometer can detect slight changes in the magnetic and gravitational field of the earth, which then can be compared to a map. In some IMUs pressure and temperature sensors were installed, collecting data that can be used to calculate the air density [35]. One technology that is currently used to share the position of the aircraft with others is FLARM. It uses GPS and radio signals to communicate and is very lightweight [36]. To prevent any crashes with obstacles or other aircraft, “PEL-E-FAN-T“ has a variety of distance measuring sensors to detect critical situations or possible crashes as soon as possible. A sensor that is very common in robotics is the sonar. It is the cheapest of these distance measuring sensors but only has a range of several meters [37]. These sensors are used for the autonomous landing of UAVs [38]. A larger range with 250m and a detection angle of up to 270°[37] LiDAR provides a very accurate but expensive method of measuring distances [39]. To detect other aircraft on a larger scale, radar is being used. It has a range of several kilometers and enables the UAV to detect unknown aircraft and calculate an effective way to change its flight path. To give the GO an image of the situation on-site “PEL-E-FAN-T“ is equipped with several cameras for visible light, this way a 3D image can be produced and distances can be measured, and also the size of the observed object. Such cameras as well as the software are already being used in aircraft [37]. An Infrared camera provides night vision and can be used to detect heat sources, for instance, fires or pockets of embers that usually would not be seen. These high-resolution infrared cameras are used by the police to search for missing or wanted persons [40]. A possible use for the search and rescue configuration of “PEL-E-FAN-T“. The camera data can not only be used to measure the distance, size, and trajectory of an object but also to calculate the position and speed of the aircraft itself [41]. Comparing images with database landscapes can be recognized, a further way for the UAV to orient itself.

4.2.2 Software

The Data that has been collected must be processed and transferred in a fast and reliable fashion. Then the information is either fed back into the loop of autonomy or given to the operator in a user-friendly way. In [33] programs that were designed for this application were listed, some examples are “Mission Planner, QGround Control, UgCS, Horizon, and others“ [33]. Each of them must give the operator an intuitive and safe control over the aircraft. One safety feature that is provided by these programs is the "return-home-function“. Once implemented the aircraft will return to the home base or a predefined position, fully autonomous. In case the aircraft loses its connection to the operational base for a longer period, it will automatically implement this program on its own. Small UAVs, such as the DJI Mavic 3, already have this feature and they work reliably [42]. Using the kinetic data, collected by the IMU, "PEL-E-FAN-T" can fly through possibly rough weather and wind conditions and keeps a steady course and altitude due to advanced software. To increase the efficiency of the UAS, area maps are provided in a shared cloud and then loaded into each aircraft before each mission. These maps help the UAV orientate itself in known areas. They can be updated by every aircraft and shared among each other [37]. These updates

can be temporary, for instance, a foreign aircraft with a certain trajectory has been spotted, or long-term, for example, there is a new building being built. In the fire fighting scenario information about water sources and fires can be shared, laying the foundation for a global firefighting strategy. This data is being shared among the fleet, as well as orders and further information provided by the ground control, giving a certain redundancy in case an aircraft loses the global connection for a brief time. UAVs and operators communicate using radio signals and internet links. In the context of this paper, no detailed software will be discussed.

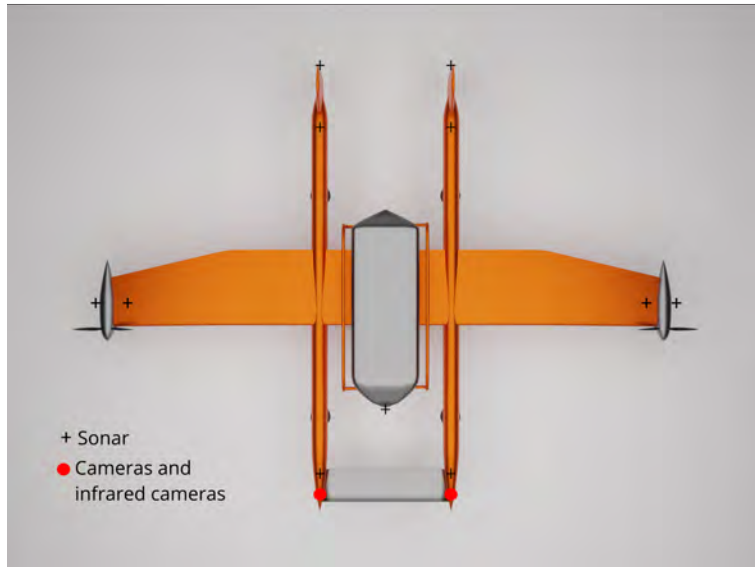


Figure 7: bottom view with sensors

5 Operational Concept

5.1 Fleet Size

The required size of the fleet is directly related to the amount of water that each aircraft can transport. Furthermore, it is necessary to consider that an optimal fleet size for each type of firefighting aircraft in terms of maximum takeoff mass, range and airspeed exists. These factors are analyzed for different types of aircraft in this paper [43]. According to the paper, 10 aircraft matches an optimum for the fleet in the case of an aircraft like the PEL-E-FAN-T. The required minimum amount of water to be transported to the fire in a single air attack is 11000l which is precisely met by the system with a water modul volume of 1100l.

5.2 Fleet-Type

It is a homogeneous one, where at the beginning of the air attack two of the ten drones fly ahead without an attached module to do reconnaissance operations to discover the water sources and memorize the ways to get there. While the first two are starting the return route, the remaining 8 head towards the fire for the first water drop. After the reconnaissance drones return to the base, they attach a tank module, which makes the fleet homogeneous even in terms of the modules, turn back to the fire and complete the first air attack. It remains to mention that in cases where people's lives are in direct danger from the fire and extinguishing would take too much time, the use of an evacuation module would make sense. In this scenario, there will be an additional evacuation module attached to an eleventh drone, making the fleet heterogeneous in terms of modules. The use of a completely homogeneous fleet provides several valuable key benefits for the user. These include low material and maintenance costs, which are achieved by uniform testing as well as lower storage costs and standardized building plans for the fleet. Furthermore, the production of a homogeneous fleet can be standardized, which minimizes time and effort. Last but not least, there are savings in terms of pilot training, because the control system does not change, and pilots only have to learn one concept, which ensures the continuous availability of pilots.

5.3 Tactics

5.3.1 Traditional Tactics

The general tactics have already been mentioned in the previous section, but should now be repeated and specified in more detail. As soon as the location of the fire is known, two reconnaissance aircraft are deployed, equipped with modules for exploring small water sources in the surrounding area. Simultaneously with the reconnaissance of the fire location and the water reservoir, the flown route is saved in the fleet's central management system so that it can be used in the following air attack. This makes it possible to put the aircraft on a kind of autopilot during en-route flights to collect water and return to the operational base for refueling or loading. After the beginning of the return of the reconnaissance aircraft to the operational base, those already equipped with water tank modules start in the direction of the fire for the first air attack. This will be completed by the now returning reconnaissance aircraft, which are also equipped with a tank module. Flying without an attached module ensures higher speeds and ranges during reconnaissance and enables subsequent piecemeal autonomous use of the drones, which secures sustained use over 24 hours, and thus compensates for the supposed loss of time due to not immediately extinguishing the fire. Regarding [44], the actual extinguishing should be characterized for different terraria. In general, there are

two different ways to fight a fire from the air. These are the offensive method, where water is dropped directly on the flames, and the defensive method, in which water is rained on the dry surrounding area of the fire to control its spread. The first one is the ground fire. This form of fire involves bushes, small trees, and branches that spread over the forest floor and is often the beginning of complete fires, which will be discussed later. Accordingly, ground fires mainly result from grass, which lies around and ignites in high solar radiation in connection with dry underwood. Access to these wildfires is often very difficult for aircraft, making the method of offensive firefighting much more inefficient than the defensive method. Thus, the aircraft should primarily moisten the surrounding forest areas from the air to prevent the spread of flames, especially to the tree crowns. A special type of ground fire is area fire. This form is different from ordinary ground fires just in the type of vegetation, so primarily open grassy areas or grain fields are affected. In this case, the burning material is often extremely dry, which makes the speed of spread almost uncontrollably fast, which means the defensive method is also significantly more effective than the offensive and the surrounding areas should be watered to slow down the spread of fire and make it controllable. The next type of fire to be considered is full fire. In this case, the entire forest, i.e. ground area and tree crowns, are burning. To fight this form, it is necessary to make a distinction in terms of the height and intensity of the flames, regarding which method is the most effective in the particular case. The information about these very decisive factors will be provided by the reconnaissance aircraft. If the flames are comparatively small and most of the water will not evaporate after dropping due to the intense heat, the offensive method will be the most efficient. However, in cases where the heat produced by the flames becomes too high, it is significantly more effective to moisten the surrounding forest, which means using the defensive method. An extraordinary case might be a fire where the surrounding area is blocked by buildings or something else. An example of this could be urban fires, such as those in California. Those should be fought aggressively to minimize the damage. At least mountain fires should be considered. It is important to know that they spread faster uphill than downhill because of the direction and the thermal effect of the flames. In addition, the upward flow of hot air caused by the fire dries the vegetation above the burn, making it even more flammable. Accordingly, the fire uphill should be fought with the defensive method, since the intensity of the flames is high in this area and the previously mentioned drying out should be counteracted. Simultaneously the fire downhill should be controlled with the offensive method, because of the increased danger for the ground troops due to rolling down glowing embers or other burning parts of the forest.

5.4 Ground Handling

For parking and quick launching of our aircraft, it is important to have access to an electric charging station and fuel. Furthermore, a storage area is needed which protects the aircraft from environmental influences. Finally, access to large amounts of water must be guaranteed at all times for filling the water modules. These requirements suggest that the operational base does not necessarily have to be an airport since the takeoff run is not essential due to the VTOL characteristic of our aircraft. Therefore, larger warehouses or other large-scale buildings could also be used as a stationing location, which simplifies the wide-area coverage of a forest fire endangered region with firefighting aircraft immensely, due to the resulting shorter distances to the fire. Another consideration would be to position small sensors permanently in these regions at risk of forest fire, whose information would then be picked up by the reconnaissance aircraft to improve the early detection of the fire even further [45]. Concerning the actual control, it is planned that this will be done from the operational

base and executed by a pilot. He will sit in a control station similar to a cockpit, in which are several screens that will be supplied with information and images from the sensors and cameras of the aircraft. By placing the video recording devices at optimal locations, for example on the nose of the aircraft, the pilot has an unrestricted view of what is happening on the ground, which allows him to perform an ideal firefighting attack. The aircraft itself is controlled by satellite, which eliminates range limitations. In the military, this method has been used for several years, so it has already been sufficiently tested (for example the MQ-9 Reaper). Another advantage of this control method will be the possibility to build or expand a central base from which each aircraft can be controlled. This makes it unnecessary to set up the required control facilities at each airbase, which saves a lot of money. If the drones are all needed in one place, it is planned that they fly without modules from their stationing airports to the operational base to maximize the range. They will be delivered by train, for example. Furthermore, the use of a control center provides logistical advantages, as the number of pilots each country needs can be reduced immensely a readiness system can be realized significantly easier and more comfortable for the pilots since they could relocate their residences near to it. In this concept, the tasks of the pilots are divided into flying firefighting attacks and refueling the modules. In concrete terms, two are supposed to actively extinguish the fire, one should observe the drones during refueling and intervene in case of emergency, and the fourth is a reserve in case the others are overwhelmed. One cycle in the firefighting attack lasts 17 minutes, which means that for 10 aircraft, a refueled aircraft arrives every 100 seconds. Thus, one of the two firefighting pilots receives a new drone every 3 minutes and has one minute to drop the water before the next one arrives. The routes taken by these aircraft on autopilot were flown in advance by the reconnaissance aircraft and stored in the central memory of the control system. Due to this distribution, it is possible to reduce the number of pilots once again, as only 4 pilots are needed to transport 11000 liters. Consequently, it is possible to achieve a continuous firefighting operation of 24 hours with a team of 12 pilots and an 8-hour shift system. It should be mentioned that the eight hours are not planned in one piece they are distributed over the 24 hours in blocks between 1 and a maximum of 4 hours. Each pilot would have a rest period of 16 hours each day, which is a significant reduction in workload compared to current standards. Another advantage would be the savings in salaries for the pilots since significantly less would be needed. Furthermore, the "PEL-E-FAN-T" can support ground forces not only by airdropping but also by delivering further modules by using the cargo variant. As support modules, for example, those of the company frontline [46] would be thinkable.

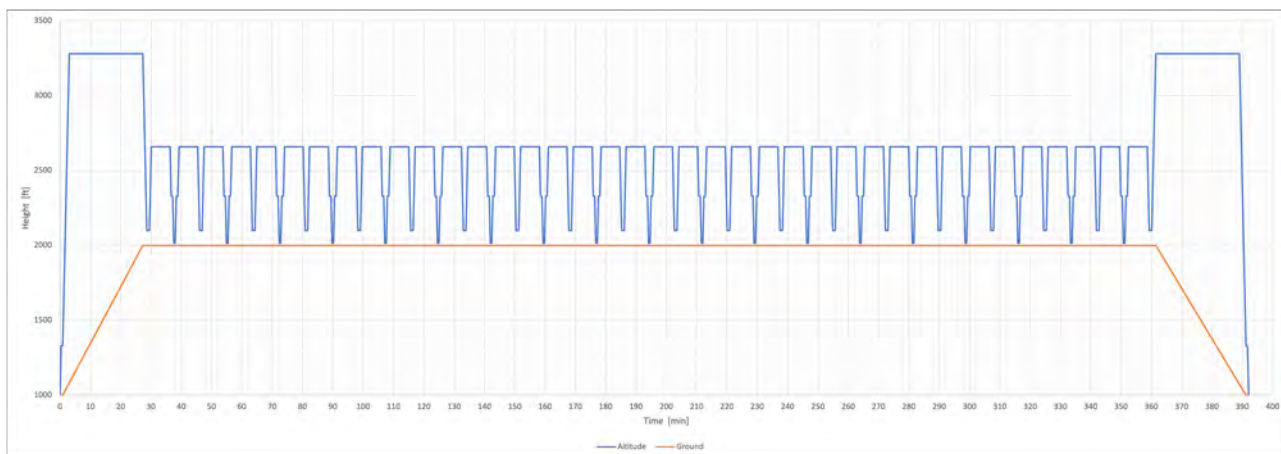


Figure 8: Mission profile

5.5 Design Mission

The design mission would begin with the deployment of two of the ten aircraft without an attached module to scout and memorize the routes later flown during the firefight. These routes include the distance of 75NM between the operational base and the fire, as well as those 15NM to small water sources. After completing this task and having sufficient information such as the area spread, height, and intensity of the flames, the reconnaissance drones will return to the operational base. Simultaneously with the start of returning flight, the remaining 8 aircraft, which had been prepared for the mission during the time since the fire was reported, will be deployed. After reaching the scene of the fire, they split up and begin the first drop. Afterward, they head to the small water sources to refill their modules. When they reach the area, a transition from horizontal to vertical flight is planned, followed by a vertical descent realized by the 6 vertical rotors. The filling of the tank module will finally be performed in hover flight, which is followed by another transition from vertical to horizontal flight. Simultaneously with their return to the fire, the two aircraft, which were previously used for reconnaissance and now also have a water module attached, reached the fire to complete the first firefighting attack. Afterward, these two also head to the small water sources for refueling, while the remaining 8 already start the second firefighting attack. This sequence is maintained until the first aircraft has to return to the operational base for refueling. Because the drones were sent at a certain time interval, this moment does not occur at the same time, so as the firefighting operation progresses, a situation arises in which some aircraft are collecting water from small sources, and some are on their way back to the operational base to refuel, and the rest are fighting the fire. Consequently, there will never be a situation in which either all of them are fighting the fire or none of them are. This permanent fighting ensures that the fire does not have a chance to recover, which makes it more controllable on the one hand and the whole process much more effective on the other. In addition, this procedure can be implemented permanently over 24 hours due to the shift system for the pilots already mentioned in the point on ground management.

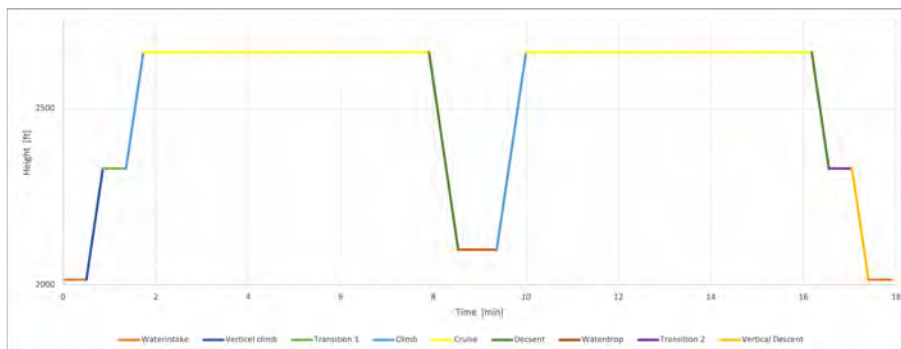


Figure 9: Mission profile in detail

5.5.1 Inland Scenario

The „PEL-E-FAN-T“ can operate perfectly in an Inland-Scenario, because it is designed to use even the smallest lakes for water intake, which makes it very efficient. The Procedure is similar to the one described at Tactics, starting with the deployment of 2 reconnaissance drones. Those will head directly to the fire source, split up and circle the affected area transferring the flown route to the central control system. After surrounding the area, the drones will start searching for nearby stretches of water and transmit those coordinates completing the route. Finally, they head back to the operational base where they get equipped with a tank-module to complete the fire attack the other eight drones have already performed. The fire fighting will be done continuously without interruption due to the pilot’s shift system as explained in “Ground Handling”. The procedure will always be in accordance with the Design Mission. As a specific example for an Inland-Scenario the fire in Jüterbog in Brandenburg will be looked at. In 2019 the fire broke out on a former military exercise area and quickly spread out, setting 750 hectares of forest and meadow alight. There can be found several smaller lakes not wider than 150 meters in a radius of 10 kilometers around the area, where it won’t be possible for conventional air tankers to fill with water. They will have to fly more than twice the range to reach a water source big enough for a scooping-maneuver. The „PEL-E-FAN-T“ is perfectly designed to use even the smallest lakes for water intake due to its “pump snorkel” and hover ability, making the firefighting even more efficient. For the sake of simplicity, the drones will start from the Leipzig/Halle airport located 90 kilometers away from the fire, also being able, in case of a longer lasting firefight, to be stationed at a smaller local airfield, as soon as the needed components were brought there.

5.5.2 Seaside Scenario

The fire in the Costa del Sol tourist area in the Sierra Bermeja mountain region near Malaga will be used as an example to illustrate the concrete procedure of a firefighting operation. Back in 2021, fires caused devastation there and destroyed 9.000 hectares of forest [47]. This year the area burned again and caused great damage since the area is difficult to access for ground troops due to the heavy vegetation, which makes the use of the "PEL-E-FAN-T" justifiable. In this case of operation, it might be worth considering the possibility of equipping the area with the small sensors for early detection already mentioned in the point "Ground Handling", since fires rage here almost every year and the danger posed by them can be significantly limited as a result. Furthermore, the pilots will be guaranteed a better view of

the fire with a simultaneous immense reduction of the danger and the stress. For simplicity, the drones would be stationed at Malaga Airport, which is just under 100km away from the fire. It is planned that the basic sequence of the firefighting attack is the same as in the design mission, with the water being taken mainly from the Mediterranean Sea, which is only about 10km away. In the direction of the sea, there are several small water sources along the rivers "Arroyo de Enmedio" and "Arroyo Vaquero", which could be approached by a configuration without "sea-snorkel" and could be made usable as well, which would reduce the distance between water intake and drop even more. In terms of effectiveness, in this scenario, the fleet is heterogeneous in terms of modules. Nevertheless, nothing changes for the pilots' control except that the fourth will have to temporarily intervene due to the increased probability of overload for the remaining three.

5.6 Further Uses

Outside of various firefighting missions, the "PEL-E-FAN-T" is suitable for agricultural field watering, as an air taxi, for mountain rescue, and as a drone for delivering packages. Because of the extinguishing lance, which is included in the water module, it is possible to extinguish an urban fire in cases where the drone has enough space to manoeuvre since her wingspan is 17m.

6 Cost Estimation

6.1 Life Cycle Costs

Predicting the Lifecycle costs of an aircraft is particularly difficult in times of economic uncertainty. Empirical formulas of a modified DAPCA IV Cost Model, called the Eastlake model, are used [48]. Correction factors for the development of composite aircraft are applied. All calculated costs and salaries are adjusted for inflation. Finally, the engineering, avionics and flight-test operation costs got increased by 100%, 50% and 10%, respectively, to account for the more complex remote control system, autonomous flight capability and additional testing and development required for the different modules and their systems. Battery prices are projected to be between 200-250\$ per kWh [49] [24]. It is assumed that 150 aircraft will be built over a five-year period. With these parameters in mind, one aircraft is expected to cost 15.8 million dollars with a 10% profit margin. The yearly operating costs amount to around 756.100 dollars, assuming a yearly flight time of 1500 hours, and a pilot salary of $150 \frac{\$}{h}$. The fuel cost is estimated to be around $2.22 \frac{\$}{gal}$ based on the assumption that the increase in fuel cost matches the increase in oil prices stated in an RC-EU-TIMES report [50]. According to this report, the oil price is likely to increase by 46 % from the 2015 level, up until 2030. It has to be mentioned though, that current fuel prices are much higher. The plane is designed to fly mostly autonomous and requires only minimal attention from an external pilot. One pilot is able to supervise three aeroplanes at a time, which massively decreases crew costs.

6.2 Impact of Autonomy

High-performance systems lead to increasing costs of purchase, the cheapest way to realize the sensor system would be using cameras[Andert - Schon als Quelle vorhanden]. A great part of the costs will be compensated by the sinking personal costs, saving about 75% of the crew. Also, the fact that every firefighting attack is at the same time a reconnaissance flight, leads to a saving of costs for further aircraft and their operation. An AI-based planned route and firefighting will make the PEL-E-FAN-T more effective and efficient [51] [52], giving it even more advantages over conventional firefighting aircraft of this size.

7 Conclusion

The challenge provided by the DLR in 2022 to design an efficient, safe, cost appropriate firefighting aircraft concept can be met by many different designs. However, the PEL-E-FAN-T is the optimal solution for a modern aerial firefighting system. The VTOL capabilities combined with the efficiency in cruise flight due to the fixed wing configuration provides the aircraft with a unique package of key advantages compared to current aircraft. Furthermore the autonomous and remote control capabilities of the system eliminates the risk for the life of the pilot in dangerous flight manoeuvres during the fire attack. Due to modular design the PEL-E-FAN-T offers versatility never seen before opening up new possibilities in fire fighting and fire rescue but also provides a fast way to switch to a configuration used for generating profit in the off season, overshadowing initial costs. The PEL-E-FAN-T is more efficient, precise, safe and versatile as well as more profitable than current fleets.

References

- [1] *Forest Fires*. URL: https://ec.europa.eu/commission/presscorner/detail/e%20n/ip_22_3719.
- [2] Sihao Sun et al. “Autonomous quadrotor flight despite rotor failure with onboard vision sensors: Frames vs. events”. In: *IEEE Robotics and Automation Letters* 6.2 (2021), pp. 580–587.
- [3] P Nathen et al. *Architectural performance assessment of an electric vertical take-off and landing (e-VTOL) aircraft based on a ducted vectored thrust concept*. 2021.
- [4] Julian Hoelzen et al. “Conceptual Design of Operation Strategies for Hybrid Electric Aircraft”. In: *Energies* 11 (Jan. 2018), p. 217. DOI: [10.3390/en11010217](https://doi.org/10.3390/en11010217).
- [5] Smruti Sahoo, Xin Zhao, and Konstantinos Kyprianidis. “A Review of Concepts, Benefits, and Challenges for Future Electrical Propulsion-Based Aircraft”. In: *Aerospace* 7.4 (2020). ISSN: 2226-4310. URL: <https://www.mdpi.com/2226-4310/7/4/44>.
- [6] Mark D Moore. “Distributed electric propulsion (DEP) aircraft”. In: *NASA Langley Research Center* (2012).
- [7] Tomas Sinnige et al. “Wingtip-Mounted Propellers: Aerodynamic Analysis of Interaction Effects and Comparison with Conventional Layout”. In: *Journal of Aircraft* 56 (Nov. 2018), pp. 1–18. DOI: [10.2514/1.C034978](https://doi.org/10.2514/1.C034978).
- [8] Dr. Andreas Klöckner. “Die Zukunft fliegt elektrisch! Vom Lufttaxi bis zum Regionaljet”. In: *LUFFFAHRT – Elektrisches Fliegen* (). URL: https://www.dlr.de/content/de/downloads/2017/die-zukunft-fliegt-elektrisch.pdf?__blob=publicationFile&v=4.
- [9] glpautogas.info. *wasserstoff tankstellen in spanien auf Juli 2022*. 2022. URL: <https://www.glpautogas.info/de/wasserstoff-tankstellen-spanien.html>.
- [10] V. G. Volchenko and A. N. Ser’oznov. “Hybrid and electric propulsion system of aircrafts”. In: *AIP Conference Proceedings* 2351.1 (2021), p. 030015. DOI: [10.1063/5.0052622](https://doi.org/10.1063/5.0052622). eprint: <https://aip.scitation.org/doi/pdf/10.1063/5.0052622>. URL: <https://aip.scitation.org/doi/abs/10.1063/5.0052622>.
- [11] Gabrielle E. Wroblewski and Phillip J. Ansell. “Mission Analysis and Emissions for Conventional and Hybrid-Electric Commercial Transport Aircraft”. In: *Journal of Aircraft* 56.3 (2019), pp. 1200–1213. DOI: [10.2514/1.C035070](https://doi.org/10.2514/1.C035070). eprint: <https://doi.org/10.2514/1.C035070>. URL: <https://doi.org/10.2514/1.C035070>.
- [12] Manuel A. Sánchez R. Carlos D. Gallo M. Josselyn Anzai Alexandre H. Rendón. “Aircraft Hybrid-Electric Propulsion: Development Trends, Challenges and Opportunities”. In: *Journal of Control, Automation and Electrical Systems* (). URL: <https://doi.org/10.1007/s40313-021-00740-x>.
- [13] J.Ludowicy R.Rings D.F.Finger C.Braun. “Sizing studies of light aircraft with serial hybrid propulsion systems”. In: *Deutscher Luft- und Raumfahrtkongress 2018* (). URL: <https://www.dglr.de/publikationen/2018/480226.pdf>.
- [14] Michael Schultz Robert Brühl Hartmut Fricke. “Air taxi flight performance modeling and application”. In: *2021* ().
- [15] Constantin Rotaru and Michael Todorov. “Chapter 2 Helicopter Flight Physics”. In: 2018.
- [16] J. G. Leishman. “Principles of Helicopter Aerodynamics”. In: *2000* ().

- [17] Equipmake. “Data Sheet Ampere-220”. In: 2022 ().
- [18] Jae-Hyun An et al. “Advanced Sizing Methodology for a Multi-Mode eVTOL UAV Powered by a Hydrogen Fuel Cell and Battery”. In: *Aerospace* 9.2 (2022). ISSN: 2226-4310. URL: <https://www.mdpi.com/2226-4310/9/2/71>.
- [19] EASA. “TYPE-CERTIFICATE DATA SHEET PrattWhitneyCanada PT6C-67 series engines”. In: (2012).
- [20] *Rolls-Royce unveils its new 'turbogenerator' with a new small engine*. URL: <https://interestingengineering.com/rolls-royce-turbogenerator-engine>.
- [21] CAL FIRE. “Firefighting Aircraft Recognition Guide”. In: 2019 ().
- [22] Global Helicopter Service GmbH. “AIRCRAFT SPECIFICATION SHEET BELL 212 - D-HEPP”. In: (2022).
- [23] Xueyan Huang et al. “Comprehensive evaluation of safety performance and failure mechanism analysis for lithium sulfur pouch cells”. In: *Energy Storage Materials* 30 (2020), pp. 87–97. ISSN: 2405-8297. DOI: <https://doi.org/10.1016/j.ensm.2020.04.035>. URL: <https://www.sciencedirect.com/science/article/pii/S240582972030163X>.
- [24] C. Pornet and A.T. Isikveren. “Conceptual design of hybrid-electric transport aircraft”. In: *Progress in Aerospace Sciences* 79 (2015), pp. 114–135. ISSN: 0376-0421. DOI: <https://doi.org/10.1016/j.paerosci.2015.09.002>. URL: <https://www.sciencedirect.com/science/article/pii/S0376042115300130>.
- [25] Chen Yang et al. “Approaching energy-dense and cost-effective lithium–sulfur batteries: From materials chemistry and price considerations”. In: *Energy* 201 (2020), p. 117718. ISSN: 0360-5442. DOI: <https://doi.org/10.1016/j.energy.2020.117718>. URL: <https://www.sciencedirect.com/science/article/pii/S0360544220308252>.
- [26] Abbas Fotouhi et al. *Lithium-Sulfur Battery Technology Readiness and Applications—A Review*. 2017. DOI: [10.3390/en10121937](https://doi.org/10.3390/en10121937). URL: <https://www.mdpi.com/1996-1073/10/12/1937>.
- [27] Egbert Torenbeek. “Airplane weight and balance”. In: *Synthesis of Subsonic Airplane Design: An introduction to the preliminary design of subsonic general aviation and transport aircraft, with emphasis on layout, aerodynamic design, propulsion and performance*. Dordrecht: Springer Netherlands, 1982, pp. 263–302. DOI: [10.1007/978-94-017-3202-4_8](https://doi.org/10.1007/978-94-017-3202-4_8). URL: https://doi.org/10.1007/978-94-017-3202-4_8.
- [28] Seth B Anderson. “A look at handling qualities of canard configurations”. In: *Journal of Guidance, Control, and Dynamics* 10.2 (1987), pp. 129–138.
- [29] Eugene L Tu. “Vortex-wing interaction of a close-coupled canard configuration”. In: *Journal of aircraft* 31.2 (1994), pp. 314–321.
- [30] Arlind Pape. *Analyse der neuen LTH-Methode zur Massenschätzung von Flugzeugbaugruppen*. 2019. DOI: [10.7910/DVN/VIOW4X](https://doi.org/10.7910/DVN/VIOW4X). URL: <https://dataverse.harvard.edu/citation?persistentId=doi:10.7910/DVN/VIOW4X>.
- [31] Karl D Bilimoria, Walter W Johnson, and Paul C Schutte. “Conceptual framework for single pilot operations”. In: *Proceedings of the international conference on human-computer interaction in aerospace*. 2014.
- [32] *Amazon darf Drohnenzustellung testen*. URL: <https://www.tagesschau.de/wirtschaft/amazon-drohnen-101.html>.

- [33] Ahmed Refaat Ragab et al. “WILD HOPPER Prototype for Forest Firefighting”. In: *International Journal of Online and Biomedical Engineering (iJOE)* 17.09 (2021), pp. 148–168. DOI: [10.3991/ijoe.v17i09.25205](https://doi.org/10.3991/ijoe.v17i09.25205). URL: <https://online-journals.org/index.php/i-joe/article/view/25205>.
- [34] *Mehr Genauigkeit, mehr Alltagsnutzung: Galileo*. URL: <https://www.dlr-innospace.de/innospaceexpo/M&K/Home/content/satellit.html>.
- [35] *IMU und Robotertechnik: Was Sie wissen sollten*. URL: <https://www.generationrobots.com/blog/de/imu-und-robotertechnik-was-sie-wissen-sollten-2/>.
- [36] FLARM. “Kollisionswarnungen und Verkehrsanzeigen für die Allgemeine Luftfahrt und Drohnen”. In: *2020* ().
- [37] Franz Andert. “Bildbasierte Umgebungserkennung für autonomes Fliegen”. In: *DLR-Forschungsbericht 2011-09* (Mar. 2011).
- [38] Srikanth Saripalli, Gaurav S Sukhatme, and James F Montgomery. “An experimental study of the autonomous helicopter landing problem”. In: *Experimental Robotics VIII*. Springer, 2003, pp. 466–475.
- [39] *Die wichtigsten LiDAR-Parameter – Den Durchblick behalten*. URL: <https://www.blickfeld.com/de/blog/lidar-parameter-verstehen/#Detection-Range>.
- [40] *Modernster Hubschrauber der Welt: Alarmhubschrauber H145*. URL: <https://polizei.nrw/artikel/modernster-hubschrauber-der-welt-alarmhubschrauber-h145>.
- [41] Eike Harm Otto Bremers. “Multi-Sensor Data Fusion zur optischen Navigation im Kontext unbemannter Luftfahrzeuge”. In: *2020* ().
- [42] *Mavic 3 Imaging Above Everything*. URL: <https://www.dji.com/de/mavic-3?site=brandsite&from=nav>.
- [43] Prajwal Shiva Prakasha et al. “Exploration of Aerial Firefighting Fleet Effectiveness and Cost by System of Systems Simulations”. In: *32nd Congress of the International Council of Aeronautical Sciences*. ICAS 2021. International Council of Aeronautical Sciences, 2021. URL: <https://elib.dlr.de/148125/>.
- [44] Hofmann Felix Kaulfuß Susanne. “Arten und Strategien der Waldbrandbekämpfung”. In: *Strategien der Waldbrandbekämpfung* (). URL: <http://www.waldwissen.net>.
- [45] Prajwal S. Prakasha et al. “System of Systems Simulation driven Urban Air Mobility Vehicle Design”. In: *AIAA AVIATION 2021 FORUM*. DOI: [10.2514/6.2021-3200](https://doi.org/10.2514/6.2021-3200). eprint: <https://arc.aiaa.org/doi/pdf/10.2514/6.2021-3200>. URL: <https://arc.aiaa.org/doi/abs/10.2514/6.2021-3200>.
- [46] *Professionelle Ausrüstung für Feuerwehren zur Waldbrandbekämpfung*. URL: <https://www.vallfirest.com/de/frontline>.
- [47] *Spanien: Waldbrand an der Costa del Sol – 3000 Menschen evakuiert*. URL: <https://www.stern.de/panorama/spanien--waldbrand-an-der-costa-del-sol---3000-menschen-evakuiert-31935876.html>.
- [48] Snorri Gudmundsson. *General aviation aircraft design : applied methods and procedures - [1st ed.]* Oxford, UK: Butterworth-Heinemann, 2014. Chap. 2.
- [49] Björn Nykvist and Måns Nilsson. “Rapidly falling costs of battery packs for electric vehicles”. In: *Nature Climate Change* 5 (Mar. 2015), pp. 329–332. DOI: [10.1038/nclimate2564](https://doi.org/10.1038/nclimate2564).

- [50] Neven Duić Nedeljko Štefanić Zoran Lulić Goran Krajačić Tomislav Pukšec Tomislav Novosel. “EU28 fuel prices for 2015 2030 and 2050”. In: *2017* ().
- [51] Kristian Korsvold Fettig. *Entwicklung einer optimierten Flugbahnplanungsmethode zum Zweck der Flugbereichsbestimmung für unbemannte Luftfahrzeuge*. Tech. rep. Institut für Flugsystemtechnik, Sept. 2020. URL: <https://elib.dlr.de/139523/>.
- [52] Moritz Plingen. “Künstliche Intelligenz im Luftverkehr”. In: *2021* ().
- [53] KAVAKAVIATION. “Medium Bell 28VDC High Output Hover Refill Pump”. In: *2022* ().

A Appendix

A.1 Formulas

A.1.1 power and energy demand formulas

$$DL = \frac{W_0}{n_{rotor} \cdot 2A} \quad (15)$$

$$v_h = \sqrt{\frac{W_0}{2 \cdot \rho \cdot A}} \quad (16)$$

$$\sigma = \frac{N_{rotorblades} \cdot c_{rotor}}{\pi \cdot \frac{(d_{rotor,vtol})^2}{4}} \quad (17)$$

$$v_{tip} = \frac{\pi \cdot RPM \cdot d_{rotor}}{60} \quad (18)$$

$$P_{induced} = \frac{W_0}{\eta_{trans}} \cdot \sqrt{\frac{-(v_{trans}^2)}{2} + \sqrt{\left(\frac{v_{trans}^2}{2}\right)^2 + \left(\frac{W_0}{2 \cdot \rho \cdot A \cdot n_{rotor}}\right)^2}} \quad (19)$$

$$P_{drag,rotor} = \rho \cdot A \cdot v_{tip}^3 \cdot \left(\frac{\sigma \cdot C_{D,rotor}}{8}\right) \quad (20)$$

$$P_{drag,aircraft} = 0,5 \cdot \rho \cdot v_{trans}^3 \cdot C_{D,trans} \cdot S_{wing} \quad (21)$$

$$R_{oCcl} = v_{climb} \cdot \sin(\gamma_{climb}) \quad (22)$$

$$v_{i,ld} = v_h \cdot \left[k + k_1 \cdot \left(\frac{R_{oDld}}{v_h}\right) + k_2 \cdot \left(\frac{R_{oDld}}{v_h}\right)^2 + k_3 \cdot \left(\frac{R_{oDld}}{v_h}\right)^3 + k_4 \cdot \left(\frac{R_{oDld}}{v_h}\right)^4 \right] \quad (23)$$

$$m_{eng,ff} = \frac{P_{climb,sc}}{m_{eng,spec} \cdot \eta_{em}} \quad (24)$$

A.1.2 aerodynamic formulas

$$S_{VT} = \frac{c_{VT} \cdot b \cdot S_{Wing}}{L_{VT}} \quad (25)$$

$$S_{HT} = \frac{c_{HT} \cdot \bar{C}_W \cdot S_{Wing}}{L_{HT}} \quad (26)$$

A.1.3 mass estimation formulas

$$m_{wing} = 2.20013 \cdot 10^{-4} [401.146 \cdot S_{wing}^{1.31} + MTOW^{1.1038}] \cdot \left(\frac{T}{C}\right)^{-0.5} \cdot AR^{1.5} \cdot \frac{1}{\cos(\phi_{25})} \quad (27)$$

$$m_{fus} = 12.7 (l_{fus} \cdot d_{fus})^{1.2982} \cdot (1 - [-0.008 \left(\frac{l_{fus}}{d_{fus}}\right)^2 + 0.1664 \left(\frac{l_{fus}}{d_{fus}}\right) - 0.8501]) \cdot \frac{w_{fus}}{d_{fus}} \quad (28)$$

$$d_{fus} = \frac{h_{fus} + w_{fus}}{2} \quad (29)$$

$$m_{htp} = 12.908 \cdot S_{HT}^{1.1868} \left(1 + \frac{0.1 - (\frac{T}{C})}{(\frac{T}{C})}\right) \quad (30)$$

$$m_{vtp} = 25.056 \cdot S_{VT}^{1.0033} \quad (31)$$

$$m_{pylon} = n_{PPT} \cdot 0.0131 \cdot SLST^{0.8806} \quad (32)$$

$$m_{sys} = 42.059(l_{fus} \cdot d_{fus})^{0.9414} \quad (33)$$

$$m_{fur} = 200 + 3.35(l_{fus} \cdot d_{fus})^{1.3368} \quad (34)$$

$$m_{opp} = 35.782 \cdot n_{PAX}^{1.1141} \quad (35)$$

$$m_{land} = 1.8 \cdot 10^{-3} \cdot MTOW^{1.278} \quad (36)$$

A.2 Aircraft and Mission Data

Table 5: aircraft and mission data

Data	Unit	Value
MTOW	[kg]	5670
W_0	[kN]	55.604
Λ	[-]	9.9497
d_{rotor}	[m]	3
c_{rotor}	[m]	0.2
n_{rotor}	[-]	4
N_{rotor}	[-]	2
RPM	$[\frac{1}{s}]$	$1.893 \cdot 10^3$
A	$[m^2]$	3.142
S_{wing}	$[m^2]$	30.43
l_m	[m]	2
W_L	[kPa]	1,827
b	[m]	17
v_{sto}	$[\frac{m}{s}]$	35.159
v_{sl}	$[\frac{m}{s}]$	30.675
H_w	[m]	609.6
H_{sc}	[m]	2438
$\rho (H_w)$	$[\frac{kg}{m^3}]$	1.159
n_{attack}	[-]	20
t_{fillup}	[s]	30
P_{pump}	[kW]	50
$m_{\text{eng,spec}}$	$[\frac{kW}{kg}]$	10
$E_{\text{density,kersion}}$	$[\frac{kWh}{kg}]$	11.9
S_{start}	[m]	0
S_{landing}	[m]	0

A.3 Constants

Table 6: constants

Constant	Value	Unit
e	0.77	[-]
c_{rotor}	0.2	[m]
k_d	0.44	[-]
α_{max}	12	[°]
γ_{climb}	4	[°]
S_{ratio}	1.35	[-]
$\Delta c_{a,\text{max,hld,to}}$	2.55	[-]
$\Delta c_{a,\text{max,hld,l}}$	3.35	[-]
η_{hover}	0.75	[-]
η_{em}	0.95	[-]
η_{climb}	0.73	[-]
η_{cruise}	0.7	[-]
$\eta_{\text{prop,ff}}$	0.85	[-]
η_{trans}	0.7	[-]
η_{PT6T}	0.3	[-]
R_{oDld}	-0.5	$\left[\frac{m}{s}\right]$
R_{oD}	-4.5	$\left[\frac{m}{s}\right]$
R_{oCto}	0.5	$\left[\frac{m}{s}\right]$
R_{oCvel}	4.5	$\left[\frac{m}{s}\right]$
R_{oCcl}	4.5	$\left[\frac{m}{s}\right]$
R_{oCsc}	0.5	$\left[\frac{m}{s}\right]$
k	0.974	[-]
k_1	-1.125	[-]
k_2	-1.372	[-]
k_3	-1.718	[-]
k_4	-0.655	[-]
v_{trans}	60	$\left[\frac{m}{s}\right]$
v_{cruise}	75	$\left[\frac{m}{s}\right]$
C_{L0}	0.2043	[-]
$C_{L\alpha}$	0.09538	[-]
C_{D0}	0.0176	[-]
$C_{L,\text{climb}}$	0.277	[-]
$C_{D,\text{climb}}$	0.021	[-]
$C_{D,\text{rotor}}$	0.01	[-]
$L_{D,\text{climb}}$	13.213	[-]
$L_{D,\text{cruise}}$	12.578	[-]

A.4 Equation Results

Table 7: equation results

Data	Value	Unit
v_{tip}	297.407	$[\frac{m}{s}]$
v_h	58.246	$[\frac{m}{s}]$
$v_{i,desc}$	61.362	$[\frac{m}{s}]$
v_{climb}	64.51	$[\frac{m}{s}]$
$v_{i,ld}$	57.288	$[\frac{m}{s}]$
P_{hover}	1.527	[MW]
P_{to}	1.533	[MW]
P_{vcl}	1.587	[MW]
P_{vd}	1.49	[MW]
P_{climb}	0.8	[MW]
P_{ld}	1.489	[MW]
$P_{induced}$	1.094	[MW]
P_{drag}	0.091	[MW]
$P_{drag,aircraft}$	0.299	[MW]
$P_{trans,hc}$	1.485	[MW]
$P_{trans,ch}$	1.485	[MW]
P_{cruise}	0.635	[MW]
$P_{climb,sc}$	1.209	[MW]
A	7.069	$[m^2]$
DL	0.983	[kPa]
σ	0.34	[-]
E_{to}	12.8	[kWh]
E_{hover}	241.7	[kWh]
E_{vc}	195.8	[kWh]
$E_{trans,hc}$	247.0	[kWh]
E_{climb}	49.4	[kWh]
E_{cruise}	2991.0	[kWh]
$E_{trans,ch}$	247.0	[kWh]
E_{vd}	184.0	[kWh]
E_{ld}	12.4	[kWh]
$E_{reserve}$	305.4	[kWh]
m_{eng}	186.986	[kg]
$m_{eng,vtol}$	202	[kg]
$m_{eng,ff}$	130	[kg]
m_{fuel}	727.589	[kg]

A.5 Mass aircraft components

Table 8: mass aircraft components

Subsystem	Data basis	Weight [kg]
Main Aircraft without modules		
wing mass	formula 27	668.25
fuselage mass	formula 28	501.69
horizontal tail plane mass	formula 30	50.175
vertical tail plane mass	formula 31	124.9
landing gear mass	formula 36	56.4
pylon mass	formula 32	175
power units mass (EM+turbine)	mass estimated from datasheet [17] [19]	662
systems mass	formula 33	332.79
Cargo Module		
fuselage mass	formula 28	409
furnishing mass	formula 34	240.30
Water Module		
fuselage mass	formula 28	319.15
pump module	mass estimated from datasheet [53]	45
Battery		
total mass	calculated with equations of [15]	194
Generator		
total mass	2 MW at $7.66 \frac{kW}{kg}$	326.4

A.6 Figures

High-Lift Device		Typical Flap Angle		$C_{A_{MAX}} / \cos \phi_{25}$	
Trailing Edge	Leading Edge	Take-off	Landing	Take-off	Landing
Plain	-	20°	60°	1.4 – 1.6	1.7 – 2.0
Slotted	-	20°	40°	1.5 – 1.7	1.8 – 2.2
Fowler ¹⁾	-	15°	40°	2.0 – 2.2	2.3 – 2.7
Double Slotted ²⁾	-	20°	50°	1.7 – 1.9	2.5 – 2.9
Double Slotted ²⁾	Slat	20°	50°	2.3 – 2.6	2.8 – 3.2
Triple Slotted	Slat	20°	40°	2.4 – 2.7	3.2 – 3.5

¹⁾ Single slotted

Figure 10: $C_{a_{max}}$, typical flap angles for different high-lift devices [27]

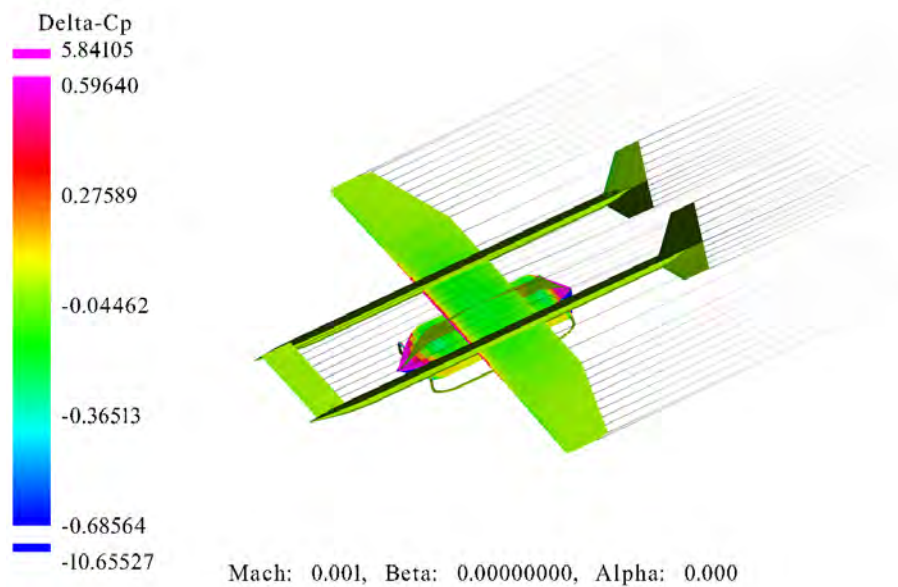


Figure 11: Drag estimation

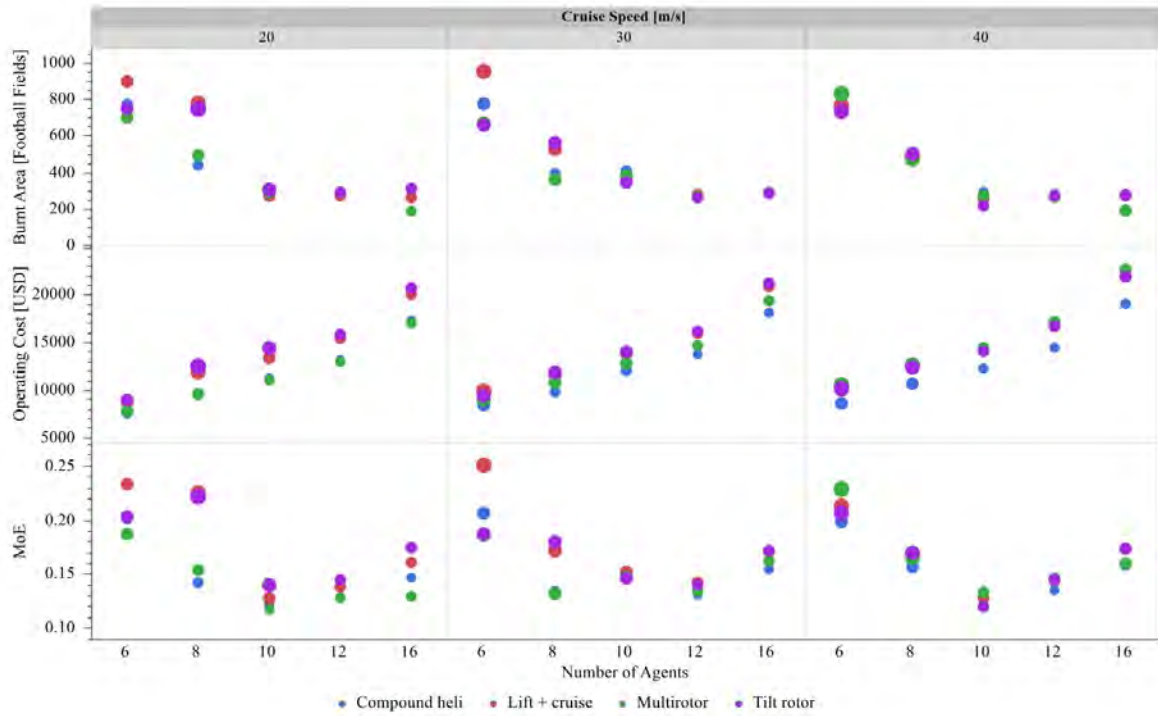


Figure 12: The sensitivity of cruise speed on the aerial firefighting effectiveness and cost. [43]

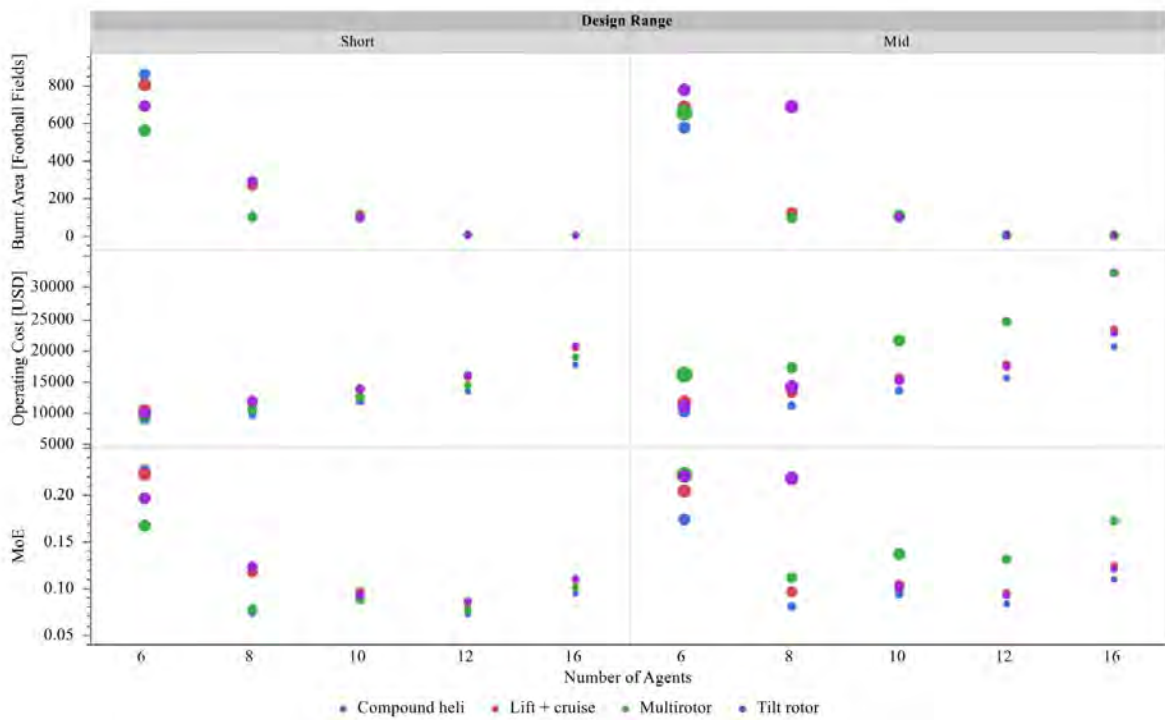


Figure 13: The impact of design range on the aerial firefighting effectiveness and cost. [43]

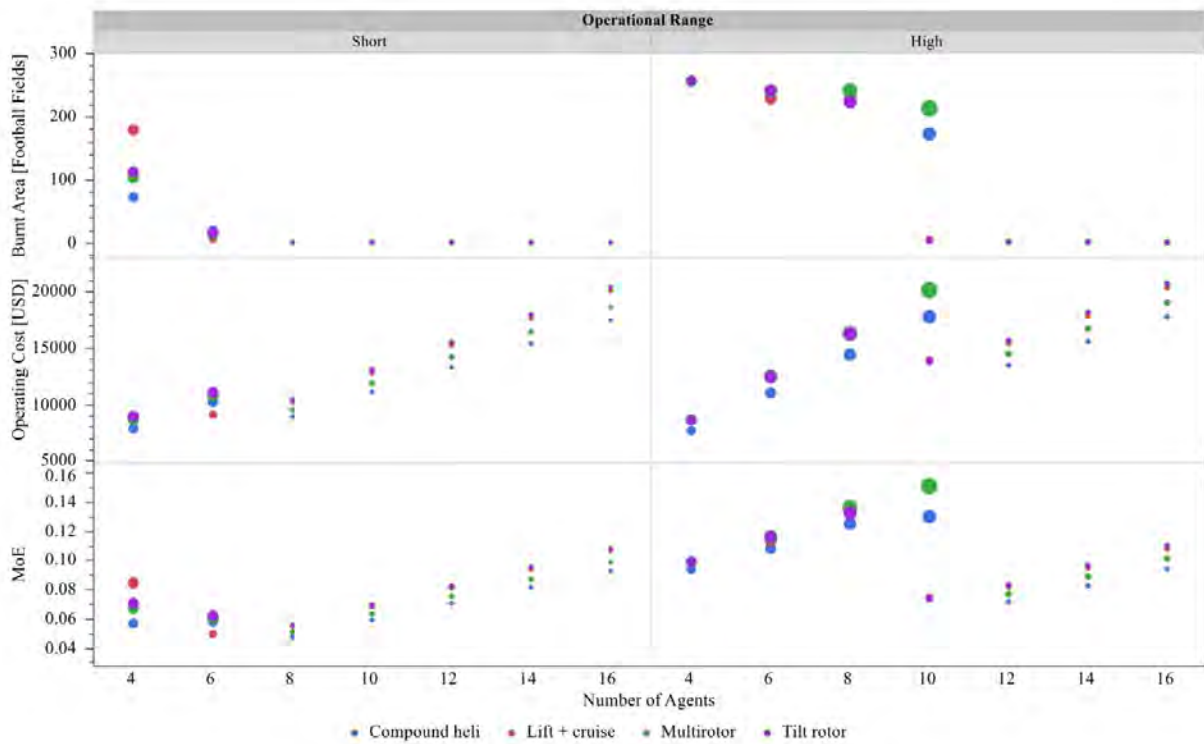


Figure 14: The impact of operational range on the aerial firefighting effectiveness and cost. [43]

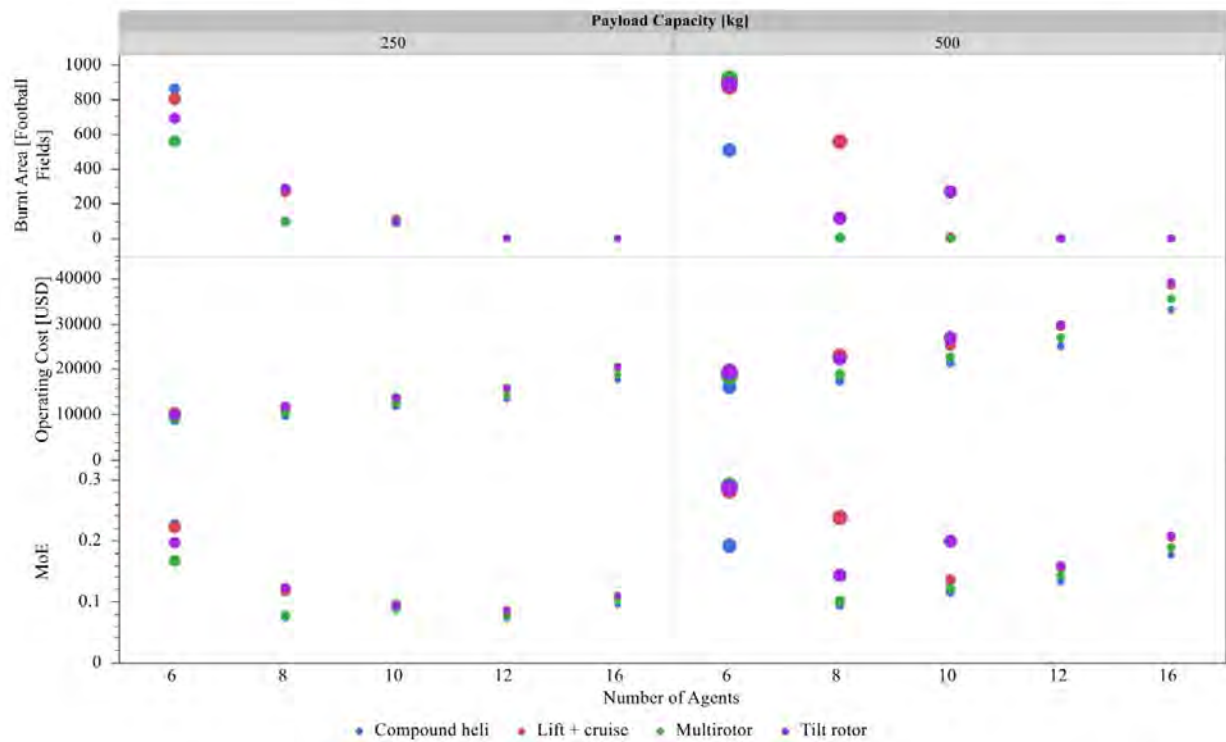


Figure 15: The impact of payload on the aerial firefighting effectiveness and cost. [43]

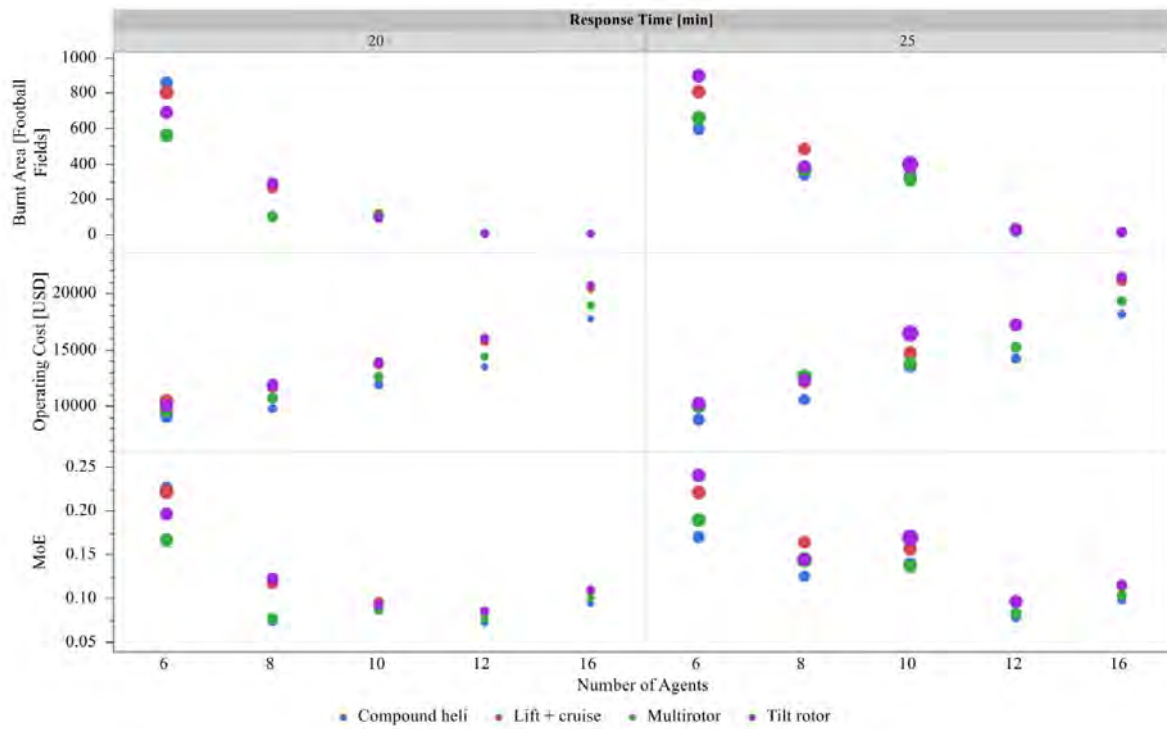


Figure 16: The impact of response time on the aerial firefighting effectiveness and cost. [43]

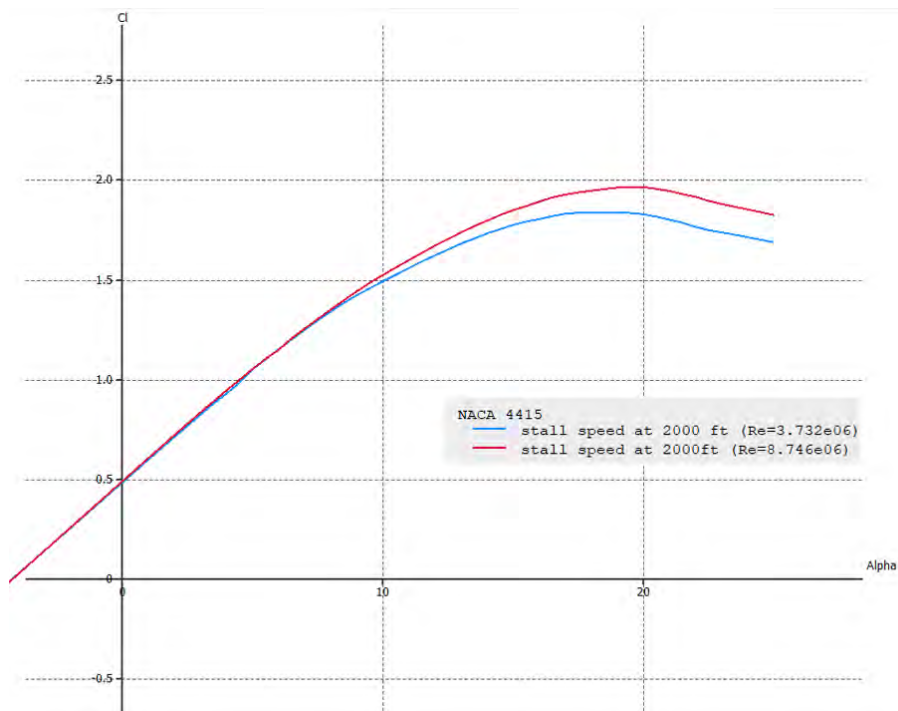


Figure 17: Naca 4415

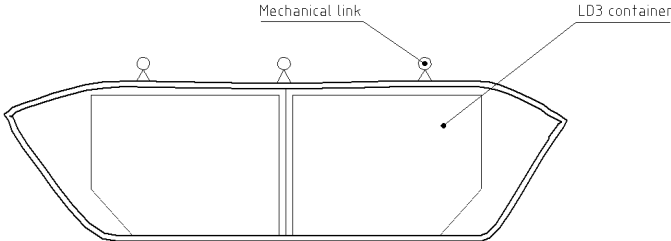


Figure 18: section view cargo module

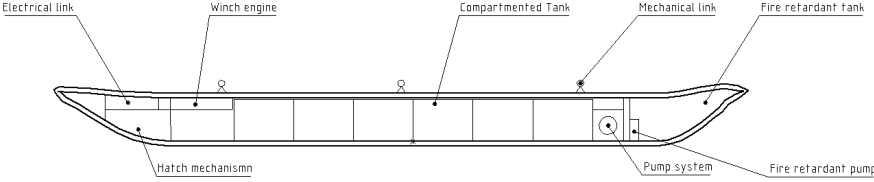


Figure 19: section view water module